

REVIEW ARTICLE

Optical halide sensing using fluorescence quenching: theory, simulations and applications—a review

Chris D Geddes¹

The Photophysics Group, Department of Physics and Applied Physics,
University of Strathclyde, 107 Rottenrow, Glasgow, Scotland G4 0NG, UK

Received 15 January 2001, accepted for publication 6 June 2001

Published 2 August 2001

Online at stacks.iop.org/MST/12/R53

Abstract

In the last century the production and application of halides assumed an ever greater importance. In the fields of medicine, dentistry, plastics, pesticides, food, photography etc many new halogen containing compounds have come into everyday use. In an analogous manner many techniques for the detection and determination of halogen compounds and ions have been developed with scientific journals reporting ever more sensitive methods.

The 19th century saw the discovery of what is now thought of as a classical method for halide determination, namely the quenching of fluorescence.

However, little analytically was done until over 100 years after its discovery, when the first halide sensors based on the quenching of fluorescence started to emerge. Due to the typical complexity of fluorescence quenching kinetics of optical halide sensors and their lack of selectivity, they have found little if any place commercially, despite their sensitivity, where other techniques such as ion-selective electrodes, x-ray fluorescence spectroscopy and colorimetry have dominated the analytical market.

In this review article the author summarizes the relevant theory and work to date for halide sensing using fluorescence quenching methods and outlines the future potential that fluorescence quenching based optical sensors have to offer in halide determination.

Keywords: halide sensing, optical sensor, fluoride, chloride, bromide, iodide, halothane, fluorescence quenching, Stern–Volmer kinetics, dynamic, static, fluorescence resonance energy transfer, multiphoton transdermal halide sensing

1. Introduction

Of the five halogens only four of them have any practical importance, of which only three, chlorine, bromine and iodine, can readily be sensed by fluorescence quenching methods. At room temperature, fluorine and chlorine are gases, bromine is a liquid and iodine a solid. The halogens are diatomic molecules in the solid, liquid and vapour states. The stability of the

diatomic species decreases with atomic number. For example, chlorine molecules are 5% dissociated at 150 °C, while iodine exists exclusively in the monatomic state at 1000 °C. Chlorine and bromine react with water quite readily, to eventually form the respective aqueous halide ions, after decomposition by light of the hydrochlorous and hydrobromous acids. The reaction only takes place to a very limited extent with iodine. The now-accepted model for the solvation of halide ions in aqueous solution is a dynamic one. At any time, the halide ion is surrounded by a first shell of oriented water molecules, their number being the primary solvation number of the ion. At large

¹ Current postal address: The Center for Fluorescence Spectroscopy, Department of Biochemistry and Molecular Biology, University of Maryland School of Medicine, 725 West Lombard Street, Baltimore, MD 21201, USA.

distances from the ion there is an unperturbed structure of bulk water, whereas in between there is a secondary solvation shell, a few molecules thick, in which the structure is modified to an intermediate extent. Where the exchange of water molecules between the primary and secondary solvation shells is slow for many transition metal ions, for halide ions the solvent exchange rates are amongst the fastest known. For example, the mean time a given water molecule is in the primary solvation shell of Cl^- is about 5×10^{-12} s (Sharpe 1990).

Inorganic halide is found in abundance in nature, found in/as minerals or as solvated halide ions by the dissolution of minerals or salts. In contrast there are relatively few naturally occurring *organic* halide compounds. This is to be expected as organic compounds take up halogens mainly by the reaction with elemental halogens or reactive halogen compounds (e.g. phosphorus halides), which themselves do not exist to any significant extent in nature. In living organisms there are a few *halogeno* amino acids, such as L- and D-*thyroxine*. In medicine we have seen halide containing antibiotics such as *chloramphenicol*, *aureomycin*, *griseofulvin* and *caldariomicetin*, the anaesthetic *halothane*, as well as many commercially made halogen compounds found in the home such as *Teflon* and the outlawed *Freon*.

In this review article the author focuses primarily on halide *ion* sensing although some methods for the determination of organic halide are briefly discussed. The author has assembled the material in such a way so as to provide both an introduction to the importance and roles of halide in the world we live, referencing many sources of halide and some of their respective determination methods, as well as providing, for the first time, a body of references which amalgamates the halide sensing work using fluorescence quenching methods, which until now have been scattered throughout the research literature.

1.1. Halide in the environment

The determination of halide concentrations in the environment is important for both monitoring *excessive* halide levels, i.e. pollution in air and waters, as well as monitoring halide *deficiencies* in natural resources, such as in soils and drinking water etc, which can, if left unchecked and remain deficient, lead to several physiological disorders. An example of each and the respective monitoring solutions are discussed below.

Chloride in the form of salt water is a major contaminant of ground water and hence its determination is important. As well as monitoring chloride levels in drinking water and for aquatic life, the monitoring of chloride diffusion into steel reinforced concrete structures, from ground water, is also important. Whilst at first this may seem merely academic, it has to be appreciated that chloride can cause corrosion of steel at concentrations as low as $600\text{--}900 \mu\text{g ml}^{-1}$ (Berke and Hicks 1993) and potentially structural failure. Salt water is also a major constituent of landfill leachate that can contaminate the ground water by dispersing through the protective landfill liners and hence the continuous monitoring of ground water halide levels is necessary. Whilst there are many laboratory methods for halide determination, relatively few can be adopted and used for the *in situ* long-term monitoring at the appropriate location (Cosentino *et al* 1995). One sensor addresses this problem by using a simple remote fibre-optic

type sensor (Cosentino *et al* 1995). This sensor works when the chloride changes a reddish-brown silver chromate strip to white silver chloride. The colour change causes the intensity of light propagating through the fibre to increase. From the predetermined calibration curve of light intensity versus chloride concentration, chloride levels can be readily obtained. The sensor was reported as being able to determine chloride in the range $100 \mu\text{g ml}^{-1}$ to greater than $3000 \mu\text{g ml}^{-1}$ with immunity to corrosion and electromagnetic interference. This was an improvement over some previous electronic sensors which were affected by corrosion and electrical surges from lightning (Cosentino *et al* 1995).

The determination of iodide and iodate in natural and wastewaters has also attracted attention in the research literature, where the concentration of iodine in seawater varies between 10^{-6} and 10^{-7} mol kg^{-1} (Sivaraman and Rajeswari 1983). The interest in iodide determination lies in the fact that iodide deficiency in natural resources is associated with the occurrence of endemic goitre in mammals (Chandramouleeswaran *et al* 1998). Hence it is important to maintain, throughout life, continual ingestion of small quantities of iodine from various feed inputs such as food and water. Analysis of such a trace quantity poses a serious problem, especially in the quantitative estimation. Microtechniques, such as colorimetry and amperometry, have been used by some workers (Barkley and Thompson 1960, Jones *et al* 1982, Sivaraman and Rajeswari 1983). The colorimetry method of Sivaraman and Rajeswari is based on the catalytic effect of iodide on the reduction of a ferric thiocyanate complex, and the measurement of the resulting fading in the intensity of the red complex using a spectrophotometer. Using this method they report a reproducibility of ± 0.0004 ppm. Colorimetry methods are amongst the most versatile for halide determination, in that many can be performed away from the laboratory using portable spectrophotometers, they are relatively simple to perform with little training required to perform the simplest of tests, they are selective and some colorimetry methods offer very good halide sensitivity indeed. Some other highly sensitive colorimetric/kinetic type methods which have been used for the analysis of halide in natural media such as water, air and rocks, include the oxidation of arsenite by cerium (Mark and Rechnitz 1968); thiocyanate by nitrite (Kreingol'd 1983); some dyes by chloramine (Yasinskene and Umbrazhyunaite 1973) and aromatic amines by hydrogen peroxide (Ghimicescu *et al* 1973), although there are many more reported in the research literature. One recent colorimetric sensor uses calixpyrroles to report the presence of halide ions by a simple color change. After future immobilization of the calixpyrroles, Gale *et al* envisage being able to produce disposable halide 'dip-sticks' for simple use away from the laboratory (Gale *et al* 1999). Several methods for the determination of iodide in the environment have been reviewed and serve as a good introduction to the topic (Butler 1996, Wong 1991).

1.2. Halide in human physiology

Most biological fluids are complicated mixtures which include inorganic electrolytes such as halide ions. In plasma and muscle cells, electrolyte composition is normally fairly

constant but in gastric/pancreatic juices, sweat, saliva and urine it may vary considerably, particularly when affected by illness. A good example of this is *cystic fibrosis*. Few diseases can be so readily diagnosed as cystic fibrosis, which is characterized by a high chloride concentration in a patient's sweat and saliva as compared to non-cystic fibrosis patients. Despite the availability of genotype determination for cystic fibrosis (Kerem *et al* 1989) sweat testing still remains one of the most important clinical and cost-effective methods. The paucity of clinical conditions associated with elevated sweat electrolytes (Wood *et al* 1976) makes this test relatively specific for cystic fibrosis. A sweat chloride testing method by pilocarpine iontophoresis, typically referred to as the Gibson-Cooke method (Gibson and Cooke 1959), was widely accepted as the standard for sweat testing, although many authors (Blick and Commens 1982, Warwick *et al* 1986, Nathanson *et al* 1994, 1995, Taylor and James 1997) have developed alternative methods for sweat chloride determination. Nathanson *et al* have shown that their microvolume method, which incorporates a chloridometer, is capable of measuring chloride concentrations in the range 9–123 mmol l⁻¹, where cystic fibrosis patients typically have chloride levels >60 mmol l⁻¹ as compared to non-cystic fibrosis individuals <40 mmol l⁻¹ (Warwick *et al* 1986).

The measurement of urinary chloride is equally as useful for the diagnosis and treatment of a variety of acid-base disorders (Winter 1981, Sherman and Faustino 1987, Preuss 1993). Urinary sodium and chloride concentrations are most often used for the assessment of effective intravascular volume. Patients with low effective intravascular volume typically have low sodium and chloride concentrations <15–25 mmol l⁻¹ (Koch and Taylor 1992, Preuss 1993). Whilst urinary sodium concentrations alone can be useful in the differential diagnosis of hyponatremia and acute renal failure, urinary chloride is useful to differentiate between saline responsive and resistive metabolic alkalosis, where a value of <15 mmol l⁻¹ urinary chloride is an indication of contracted effective intravascular volume, and, therefore suggests saline responsive metabolic alkalosis (Koch and Taylor 1992, Mersin *et al* 1995). It is interesting to note that medical decision levels for urinary sodium and chloride are significantly lower than the normal serum range.

Some published methods for chloride determination in biological samples include ion selective electrodes (Wegman *et al* 1984, Barbour 1991), ion chromatography (Yu *et al* 1996), HPLC (Tsikas *et al* 1992), clinical analysers (Melhem *et al* 1985, Komaromy-Hiller *et al* 1998), titration (Kisters *et al* 1997), cyclic voltammetry (Arai *et al* 1996) and spectrophotometry (Berry *et al* 1992).

The use of ion-selective electrodes in the determination of urinary chloride in many laboratories is common due to the advantages over some other methods in terms of their speed, cost, automation and versatility, where most electrodes can typically measure more than one electrolyte concentration. However, whilst typical sodium and potassium membrane electrodes express good linearity over a wide physiological concentration range, some chloride membrane electrodes show non-Nernstian response (Komaromy-Hiller *et al* 1998) and suffer from a series of electrolyte interferences (Wegman *et al* 1984). This, in fact, goes to the 'heart' of the problem with the use of ion-selective electrodes in medicine.

Another alternative method for chloride determination are chloride titrator strips. For many years chloride titrator strips were frequently used in nonmedical applications but have now found their way into medicine and have been used clinically as an inexpensive, accurate method of monitoring dietary salt intake (Luft *et al* 1982, Kaplan *et al* 1982, Sloan *et al* 1984). Qunatab[®] strips are simple in design, relatively cheap and allow a fairly rapid means of measuring urinary chloride. The strip consists of a 79 × 13 mm² plastic strip within which is laminated a brown capillary column impregnated with silver dichromate. When the strip is immersed in urine, the fluid rises by capillary action to a moisture sensitive band at the top of the column that signals saturation of the column by turning from orange to black. The resultant reaction of urinary chloride with silver dichromate in the column produces silver chloride, which is white. The urinary chloride concentration is proportional to the height of the white column. The titrator strips have been shown to be effective at urinary chloride concentrations in the range 25–400 mmol l⁻¹, with response times of 10–25 mins (Sloan *et al* 1984, Sherman and Faustino 1987).

Fluoride is present in biological fluids and tissues and especially in bone and tooth. Typical fluoride levels in blood have been reported to be in the range 20–60 µg l⁻¹ using a fluoride ion-selective electrode (Kissa 1987). Fluoride is easily absorbed but it is excreted slowly from the body, which can result in chronic poisoning (Michigami *et al* 1993). Fluoride has a strong effect on most enzymes and acute poisoning by fluoride is almost always caused by blockage of the enzyme functions. Hence monitoring fluoride in the human body is important. Some published methods for the determination of fluoride in biological fluids include ion chromatography (Michigami *et al* 1993); fluoride ion-selective electrodes (Seifert *et al* 1986, Kissa 1987, Tyler *et al* 1988, Tyler and Poole 1989), spectrophotometry (Culik 1986) and gas chromatography (Ikenishi and Kitagawa 1988).

The physiological significance of fluoride, chloride and iodide is well known, but bromide is still considered either as a non-essential trace element or a trace element with an unknown function (Buchberger and Huebauer 1989). However much more is known about the toxicity of bromide (Leeuwen and Sangster 1987) and hence its determination is deemed equally as important. Many authors have reported mean serum bromide levels to be in the range 2–8 mg l⁻¹, using techniques such as colorimetry and x-ray fluorescence spectroscopy (Versieck and Cornelis 1980).

Iodine is however, unlike bromine, an essential trace element in the human body (Prasad 1978). The human body contains on average 14 mg of the element, concentrated mostly in the thyroid gland. Iodine containing hormones (thyroxine, tri-iodothyronine) strongly influence a range of biological reactions. Typically, iodine species such as I⁻ and IO₃⁻ are absorbed from food and reduced to iodide (or remain as iodide) in the gastro-intestinal tract, where the absorbed iodide is considered as the main source of iodide for the synthesis of these hormones. About 1 mg of iodine per week is needed to ensure the normal synthesis of these thyroid hormones (Burguera *et al* 1996). Typical I⁻ and total iodine (organic bound + free iodide) concentrations in serum for healthy patients are in the range 2–4 µg l⁻¹ and ≈80 µg l⁻¹ respectively

Table 1. Some current methods for physiological halide determination, their range/detection limit, as reported, and typical concentrations determined in physiological samples.

Physiological sample	Halide	Measured halide in sample/s	Determination range/limit of technique	Technique	Reference
Blood	F ⁻	20–60 $\mu\text{g l}^{-1}$	0–100 $\mu\text{g l}^{-1}$	Ion selective electrode	Kissa 1987
Urine	F ⁻	2.97 \pm 0.89 $\mu\text{g ml}^{-1\text{a}}$	0.06–50.0 $\mu\text{g ml}^{-1\text{b}}$	Ion chromatography	Michigami <i>et al</i> 1993
Urine	Cl ⁻	—	\geq 5 mmol l ⁻¹	Clinical analyser	Melhem <i>et al</i> 1985
Sweat	Cl ⁻	—	2–50 mmol l ⁻¹	Clinical analyser	Taylor and James 1997
Sweat	Cl ⁻	20.9 \pm 1.9 mmol l ^{-1\text{c}}}	9–123 mmol l ⁻¹	Microvolume method	Nathanson <i>et al</i> 1994
Urine	Cl ⁻	12–276 mmol l ^{-1\text{d}}}	25–400 mmol l ^{-1\text{b}}}	Titration strips	Sloan <i>et al</i> 1984
Urine	Br ⁻	0.86–3.14 mg g ^{-1\text{e,f}}}	0.2–16 mg l ^{-1\text{b}}}	Gas chromatography	Buchberger and Huebauer 1989
Serum	Br ⁻	3.5–10 mg l ⁻¹	1.2–120 mg l ^{-1\text{b}}}	Anion-exchange chromatography	Miller and Cappon 1984
Serum	Br ⁻	1.92–2.70 mg l ^{-1\text{g}}}	0.2–16 mg l ^{-1\text{b}}}	Gas chromatography	Buchberger and Huebauer 1989
Urine	I ⁻	50–152 $\mu\text{g g}^{-1\text{f,g}}$	20–600 $\mu\text{g l}^{-1\text{b}}$	Gas chromatography	Buchberger and Huebauer 1989
Urine	I ⁻	69 \pm 39 $\mu\text{mol mol}^{-1\text{h}}$	0.1–200 $\mu\text{mol mol}^{-1\text{b}}$	HPLC	Mura <i>et al</i> 1995
Urine	I ⁻	61–125 $\mu\text{g l}^{-1\text{i}}$	\geq 10 $\mu\text{g l}^{-1}$	Head-space flow injection	Burguera <i>et al</i> 1996
Serum	I ⁻	2–40 $\mu\text{g l}^{-1}$	\geq 0.1 $\mu\text{g l}^{-1}$	Ion chromatography	Michalke <i>et al</i> 1996
Serum	I ⁻	7 \pm 5 $\mu\text{g l}^{-1\text{j}}$	$>$ 0.2 $\mu\text{g l}^{-1}$	HPLC	Moussa <i>et al</i> 1995
Urine	I ⁻	53 \pm 22 $\mu\text{g l}^{-1\text{k}}$	—	X-ray fluorescence	Turzo <i>et al</i> 1990
Urine	I ⁻	—	$>$ 0.04 $\mu\text{mol l}^{-1}$	HPLC/Ag electrode	Rendl <i>et al</i> 1994

^a Mean level and standard deviation for ten healthy persons.

^b Linear calibration region of technique.

^c Mean level and standard deviation for 111 persons. 5 μl^{-1} sweat used in the analysis.

^d Measured chloride range in 128 urine samples.

^e Range of bromide content for one test person, measured over five consecutive days.

^f The halide content in urine is expressed as a ratio of halide concentration to urinary creatinine concentration, which is typical for minor urinary constituents.

^g Range of halide levels of eight healthy persons.

^h Mean level for 30 healthy persons. ⁱ Range of iodide levels found for 100 persons.

^j Mean level for six children.

^k Mean level and standard deviation for 20 healthy persons.

—, no data.

(Michalke *et al* 1996). The determination of the total amount of iodine in biological materials has become a routine procedure (Buchberger and Winsauer 1985), whereas the determination of free inorganic I⁻ in biological samples in the presence of iodinated organic compounds still remains a problem, although there is a considerable amount of interest from the medical viewpoint.

Early methods for the determination of iodide in serum and urine were either not free of interference, such as the measurement of total iodine after ultrafiltration (Postmes and Coenegracht 1972, Globel 1977) and the use of iodide selective electrodes (Cooper and Croxon 1983), or were not suited for routine laboratory analysis, such as ¹³¹I labelled serum (Makowetz *et al* 1966, Muller 1967) and neutron activation analysis (Aabech and Steinnes 1980). More recently, methods describing the selective determination of free I⁻ in serum, plasma and urine, in the presence of organic iodine containing compounds, have been reported (Buchberger and Winsauer 1985, Buchberger and Huebauer 1989, Michalke *et al* 1996). Michalke *et al* have used ion chromatography, since this can be specific to I⁻, the lower determination limit of their procedure being 0.1 $\mu\text{g l}^{-1}$, 0.8 nmol l⁻¹, which is more than 20 times lower than normal physiological I⁻ levels.

Table 1, which is meant to be informative rather than exhaustive, summarizes some published methods for

physiological halide determination, their range and the typical halide concentrations reported for some physiological samples.

1.3. Halide in consumer products and industrial processes

The range of uses of halide and its determination in consumer products and industrial processes is vast, reaching to areas such as toothpastes and dental products (Potter *et al* 1986, Hattab 1987, 1989, Sandulescu *et al* 1996), the determination of halide in vegetation (Vijan and Alder 1984), bromide and iodide determination in milk sources (Lawrence *et al* 1983, Goewie and Hogendoorn 1985), pharmaceutical products (Abramovic *et al* 1993, Risley *et al* 1996), the monitoring of halide as a pollutant in industrial wastes and waste waters (Riggin *et al* 1984, Bryant *et al* 1990) and the determination of halide in food products such as cheese, wines and vinegars (Gonzalez *et al* 1991, Garcia *et al* 1992), to name but a very few.

One particular industry, where halide is an important control parameter and which therefore depends on its accurate determination, is the photographic industry. Silver halide photography began over 160 years ago by Jacques Daguerre, who in 1839 invented the 'daguerreotype', using a thin layer of silver iodide as a photosensitive material (Eder 1945, Suptitz 1996). It is estimated that the huge progress in silver halide materials since its discovery affords present photographic materials over one million times more sensitive than the

daguerreotype (Tani 1995). However despite its success, the future of silver halide photography is now uncertain because of the continuing improvement of CCDs (charge coupled devices), where CCD imaging *also* has the sensitivity and resolving power for taking pictures, but has the added advantage of not requiring processing with solutions that contain active chemicals and halide, that are difficult to handle and pose real threats to the environment (Tani 1995, 1998). As a result, the photographic industry is amongst the many industries *worldwide*, continually seeking highly sensitive methods for the detection and determination of aqueous halide. In recent years, one approach that has successfully been used is the quenching of fluorescence.

2. Optical halide sensing using fluorescence quenching: theory and simulations

Optically excited luminescence is generally thought of as the emission of light from an electronically excited state and is divided into two categories, *fluorescence* and *phosphorescence*, depending on the electron's conformation in the excited state. In excited singlet states, S_n , the electron in the excited orbital is paired with respect to the second electron in the ground state orbital, i.e. is of opposite spin. The return to the ground state, $S_1 \rightarrow S_0$, is spin allowed and occurs very rapidly by the emission of a photon, i.e. *fluorescence*. In contrast, when the electron in the excited orbital has the same spin orientation as the ground state electron, the transition to the ground state, $T_1 \rightarrow S_0$, is spin forbidden and the emission of the photon is relatively slower, i.e. *phosphorescence*. Since phosphorescence is 'long lived' it is not normally observed in fluid solution at room temperature, whereas fluorescence is commonly observed from fluid solutions in the absence of a quencher. This is because many deactivation processes compete with emission, such as non-radiative quenching processes (figure 1). It is these fluorescence and phosphorescence quenching processes that allow us to quantitatively sense halide.

2.1. The theory of dynamic fluorescence quenching

It is generally known that the fluorescence of certain heterocyclic indicators such as those based on quinine (Verity and Bigger 1996, Mayrhofer and Betts 1998), 6-methoxyquinoline (Urbano *et al* 1984, Krapf *et al* 1988, Geddes *et al* 1999a, b, 2001a, b, Jiwan and Soumillion 1997), anthracene (Mac *et al* 1991, Zhang *et al* 1997), naphthalenes (Behera and Mishra 1993, Behera *et al* 1995a, b), coumarins (Moriya 1984, 1986, 1988), fluorescein (Naim *et al* 1986), pyrene (Castano *et al* 1983, Deumie *et al* 1995), rhodamines (Geddes and Douglas 2000, Geddes 2000a) and various other polynuclear/heterocyclic aromatics (Davis 1973, Najbar and Mac 1991, Momin and Narayanaswamy 1992, Sarpal and Dogra 1994, Carrigan *et al* 1996) are quenched by halides and some *pseudohalides*. The resulting decrease in fluorescence emission intensity or lifetime can be measured and related directly to the halide concentration via different quenching models that the author will describe. The determination of halide using fluorescence quenching is a popular technique due to both the high sensitivity that fluorescence has to offer

(single molecules can now be detected—Lakowicz 1999) and the simplicity of quenching reactions: where only a small volume of sample is required; the reactions are usually non-destructive and the reactions can be applied to almost any system that has an extrinsic or intrinsic fluorescence probe.

There are many forms of fluorescence quenching (Eftink 1991, Lakowicz 1999). The quencher may be an electron donor, and the excited state may be the acceptor (Labiana *et al* 1972). The quenchers may act by a fluorescence resonance energy transfer mechanism (FRET), a non-radiative process where fluorescent donor and acceptor spectral overlap exists (Förster 1948, Clegg 1996, Lakowicz 1999) or the quencher may be a collisional quencher. In this case the fluorophore is returned to the ground state during a diffusive encounter with a quencher, within the lifetime of the excited state of the fluorophore, without the emission of a photon (figure 1(A)). For collisional quenching the molecules are not chemically altered in the process.

For halide, some *pseudohalides* and some other heavy atoms, quenching is thought to be a result of intersystem crossing to an excited triplet state, promoted by spin-orbit coupling of the excited (singlet) fluorophore and the halide upon contact. Since emission from the triplet state is slow, the triplet emission is likely to be quenched by other processes (figure 1(B)) (Cowan and Drisko 1970, Watkins 1974, Turro 1991, Lakowicz 1999).

Other quenching mechanisms include static quenching, where fluorophores form non-fluorescent complexes with quenchers, a process which does not rely on diffusion or molecular collisions. Quenching can also occur via many trivial processes, such as attenuation of the excitation light by the fluorophore itself or other absorbing species. Except for energy transfer and these trivial processes, the quenching mechanisms involve very close contact between the excited state of a fluorescent species and the quencher and are sometimes referred to as contact quenchers.

2.1.1. The Stern–Volmer equation. The fluorescence quenching of a fluorophore by halide was first described by George Stokes² as early as 1869 when he observed that the fluorescence of quinine in dilute sulphuric acid was reduced after the addition of hydrochloric acid, i.e. chloride ions (Stokes 1869). The process that he observed is now commonly referred to as 'dynamic fluorescence quenching', where both the lifetime and intensity of fluorescence are reduced in the presence of a quencher, Q. This process is known to follow Stern–Volmer kinetics (Stern and Volmer 1919, Weller 1961, Birks 1975) where

$$\frac{I_0}{I} = 1 + k_q \tau_0 [Q] \quad (1)$$

$$K_{SV} = k_q \tau_0 \quad (2)$$

which can be used to obtain values of $k_q \tau_0$ (the Stern–Volmer constant, K_{SV} , units M^{-1}) by plotting I_0/I as a function of $[Q]$. I_0 and I are the fluorescence intensities in the absence and presence of Q respectively, k_q is a specific constant describing bimolecular collisional deactivation of electronic energy and τ_0

² For the life, works and the discovery of fluorescence by Stokes (Stokes 1869), see Leaback (1997) and references therein.

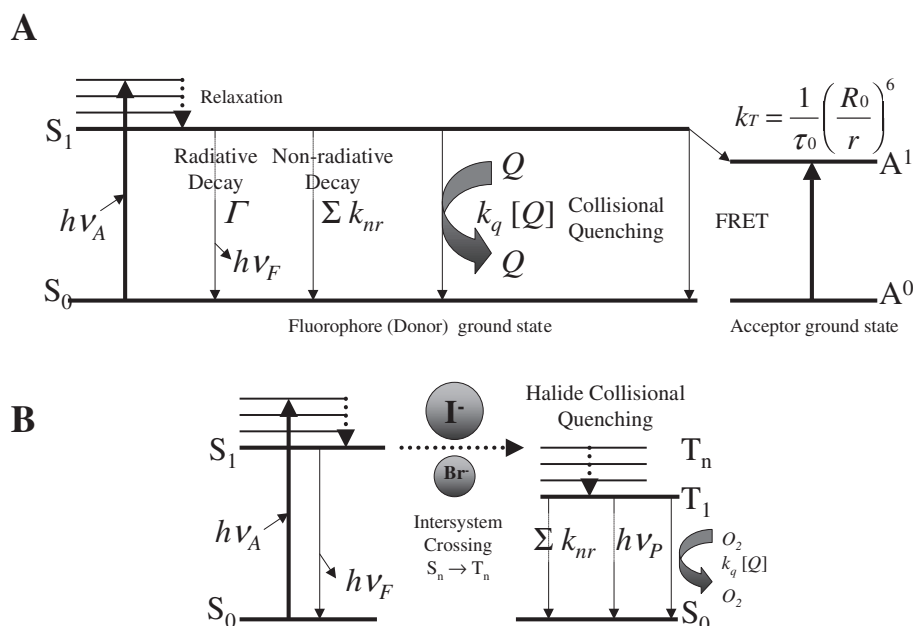


Figure 1. (A) Modified Jablonski diagram illustrating: absorption $h\nu_A$; non-radiative decay processes $\sum k_{nr}$; radiative decay, Γ , i.e. fluorescence $h\nu_F$, and other non-radiative paths to the ground state fluorescence collisional quenching and FRET. (B) Modified Jablonski diagram illustrating quenching by halide ions, where the resultant triplet state can be depopulated by: non-radiative processes; radiative decay, i.e. phosphorescence $h\nu_P$; or quenched, e.g. by dissolved O_2 .

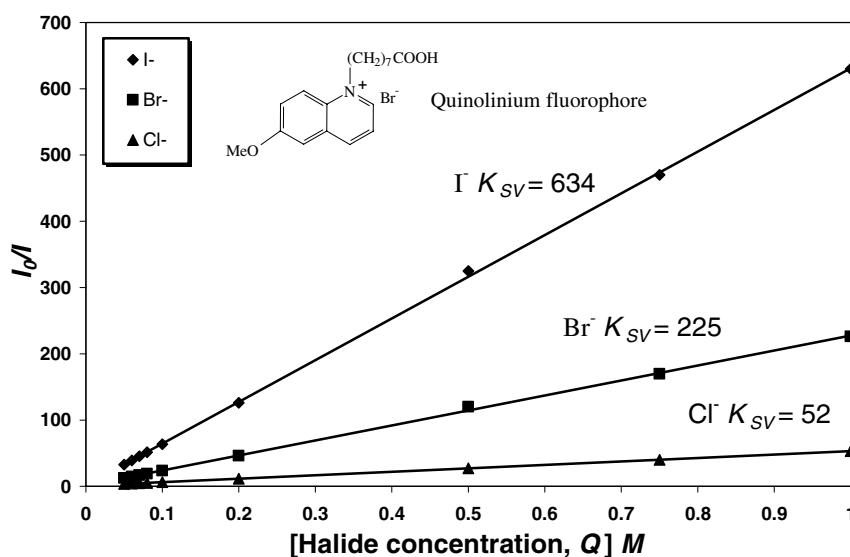


Figure 2. A typical Stern–Volmer plot, the respective K_{SV} values (units M^{-1}) and molecular structure for a quinolinium type dye quenched by aqueous halide ions at 21 °C, pH 10. (See table 2—dye E).

is the natural fluorescence lifetime in the absence of a quencher. Figure 2 shows a typical Stern–Volmer plot of a quinolinium type dye quenched by aqueous halide ions.

If quenching occurs only by a dynamic mechanism and τ_0 is a monoexponential decay time, then the ratio τ_0/τ will also be equal to $1 + K_{SV}[Q]$, where τ is the lifetime in the presence of quencher, hence,

$$\frac{I_0}{I} = \frac{\tau_0}{\tau} \quad (3)$$

This equation illustrates an important characteristic of collisional quenching, which is the equivalent reduction in fluorescence intensity and lifetime.

The dynamic or bimolecular quenching rate constant, k_q , is a useful parameter which can reflect the efficiency of quenching or the accessibility of the fluorophores to the quencher and, as will be shown later, can provide useful information on halide diffusion through polymer sensor supports. Diffusion controlled quenching usually results in k_q values $\approx 10^{10} M^{-1} s^{-1}$. Smaller values are usually indicative of shielding of the fluorophore whilst larger apparent values of k_q usually suggest some form of binding interaction (Lakowicz 1999). The bimolecular quenching rate constant is the product of the quenching efficiency, γ , multiplied by the diffusion limited bimolecular rate constant for collision, k (equation (4)),

where the value of (k) can be theoretically calculated from the Smoluchowski equation (equation (5)). The transient term has been neglected (see Eftink 1991).

$$k_q = \gamma k \quad (4)$$

$$k = 4\pi DR_0^a N^{1000} \quad (5)$$

where R_0^a and D are the sum of the molecular radii and diffusion coefficients of the quencher and fluorophore and N^{1000} is Avogadro's number divided by 1000. The factor of 1000 is necessary to keep the units correct when expressed in terms of molarity, i.e. converts molarity to molecules per cubic centimetre. Further, the diffusion coefficient for each species can be determined from the Stokes–Einstein equation:

$$D = \frac{k_b T}{6\pi R\eta} \quad (6)$$

where k_b is Boltzmann's constant, T is absolute temperature, R is the radius of the species and η is the solvent viscosity. Hence, for an efficient dynamic quencher, k_q is expected to vary with T/η . As a general rule this is true, although slight deviations from Stokes–Einstein behaviour are commonly observed (Noyes 1961). For derivations of and deviations from the Stern–Volmer equation/behaviour the author suggests the following papers and overviews: Boaz and Rollefson (1950), Keizer (1983), Laws and Contino (1992), Sung *et al* (1992, 1994) and Lakowicz (1999).

2.1.2. The 'extended' Stern–Volmer equation and its analytical implications. It was shown in 1983 that the Stern–Volmer equation can be extended to incorporate multiple solute quenchers using multiple dyes in solution (Wolfbeis and Urbano 1983). Wolfbeis and Urbano showed that the determination of n quenchers could be achieved using n fluorescent indicators, providing that the K_{SV} values were all different and that they act both dynamically and independently. This method was applied to the simultaneous determination of Cl^- , Br^- and I^- ion concentrations in a *single solution*, where standard deviations of between 3 and 5% were typically found with an improved accuracy, with increasing atomic weight of the analyte. To demonstrate that the quenching processes were independent, Wolfbeis and Urbano showed that combinations of two or three halides gave K_{SV} values that were exactly the sum of the constants of each single quencher. This paved the way for *simultaneous* halide sensing and subsequently there have been several halide sensors employing this model reported in the research literature, where fluorescent halide sensitive probes, commonly referred to as transduction elements, are immobilized in a support producing a halide sensor (Urbano *et al* 1984, Wolfbeis *et al* 1985, Zhu *et al* 1990). The author summarizes the relevant 'extended' Stern–Volmer theory.

If the fluorescence of fluorophores is quenched by multiple components present in concentrations $[Q_n]$, their contribution to the overall quenching process can be taken into account by adding additional terms to the Stern–Volmer equation.

$$\frac{I_0}{I} = 1 + {}^1K_{SV}[Q_1] + {}^2K_{SV}[Q_2] + {}^3K_{SV}[Q_3] \dots \quad (7)$$

where all K_{SV} values are Stern–Volmer constants for different indicators, and each has to be determined separately by independent plots of I_0/I against $[Q]$.

For two quencher concentrations $[Q_1]$ and $[Q_2]$ the following relationships can be given.

$$\frac{I_0^a}{I^a} - 1 = \alpha \quad (8)$$

$$\frac{I_0^b}{I^b} - 1 = \beta \quad (9)$$

where I_0^a is the fluorescence intensity of indicator A in the absence of quenchers, I^a the fluorescence intensity of A in the presence of quenchers, I_0^b the fluorescence intensity of indicator B in the absence of quenchers, and likewise I^b the fluorescence intensity of indicator B in the presence of quenchers.

Combination of equations (7)–(9) gives

$$\frac{I_0^a}{I^a} - 1 = \alpha = {}^1K_{SV}^a[Q_1] + {}^2K_{SV}^a[Q_2] \quad (10)$$

$$\frac{I_0^b}{I^b} - 1 = \beta = {}^1K_{SV}^b[Q_1] + {}^2K_{SV}^b[Q_2] \quad (11)$$

where ${}^1K_{SV}^a$ is the Stern–Volmer constant for the quenching of indicator A by the first quencher, ${}^nK_{SV}^a$ the Stern–Volmer constant for the quenching of indicator A by the n th quencher, and ${}^nK_{SV}^b$ the Stern–Volmer constant for the quenching of indicator B by the n th quencher.

Hence it follows that

$$[Q_1] = \frac{(\alpha {}^2K_{SV}^b - \beta {}^2K_{SV}^a)}{({}^1K_{SV}^a {}^2K_{SV}^b - {}^2K_{SV}^a {}^1K_{SV}^b)} \quad (12)$$

and

$$[Q_2] = \frac{(\beta {}^1K_{SV}^a - \alpha {}^1K_{SV}^b)}{({}^1K_{SV}^a {}^2K_{SV}^b - {}^2K_{SV}^a {}^1K_{SV}^b)}. \quad (13)$$

Since the Stern–Volmer constants K_{SV} are previously measured, only α and β have to be determined to calculate the quencher concentrations $[Q_1]$ and $[Q_2]$.

There are several indicators known to be quenched specifically by one quencher only. (For example rhodamine B is quenched by aqueous iodide and not aqueous bromide or chloride ions, Geddes 2000a). Therefore one of the constants in equations (12) and (13) becomes equal to zero. This simplifies the equations to give

$$[Q_1] = \frac{(\alpha {}^2K_{SV}^b - \beta {}^2K_{SV}^a)}{{}^1K_{SV}^a {}^2K_{SV}^b} \quad (14)$$

$$[Q_2] = \frac{\beta}{{}^2K_{SV}^b}. \quad (15)$$

For systems with three (or even more) quenchers, i.e. an aqueous mixture of Cl^- , Br^- and I^- ions, e.g. blood, the solution of the resulting equations becomes more difficult but can be achieved by solving the following 3×3 matrix.

$$\begin{pmatrix} \alpha \\ \beta \\ \gamma \end{pmatrix} = \begin{pmatrix} {}^1K_{SV}^a & {}^2K_{SV}^a & {}^3K_{SV}^a \\ {}^1K_{SV}^b & {}^2K_{SV}^b & {}^3K_{SV}^b \\ {}^1K_{SV}^c & {}^2K_{SV}^c & {}^3K_{SV}^c \end{pmatrix} \begin{pmatrix} [Q_1] \\ [Q_2] \\ [Q_3] \end{pmatrix}. \quad (16)$$

Again, only α , β and γ have to be measured if all K_{SV} values are predetermined.

The analytical applications of this model allows for the determination of two or more halide ion concentrations in

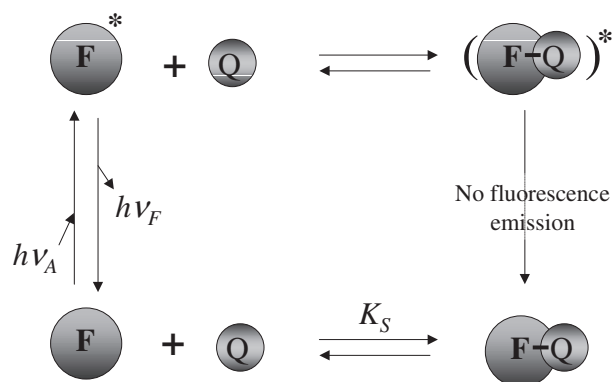


Figure 3. Static quenching. The formation of a non-fluorescent complex between fluorophore, F, and quencher Q. The static quenching constant is also the association constant for complex formation where $K_S = [F-Q]/[F][Q]$.

one solution, which is a very important consideration in physiological samples, but this model also has the added attraction of enabling interferences to be accounted for in the system under study, such as dissolved molecular oxygen (see section 2.7), provided that its K_{SV} is predetermined and that it acts independently. In effect, this model enables interferences to be mathematically described in the same way as for the halide quencher ions.

In this work Wolfbeis and Urbano have described how one (or more) fluorophores can interact with several dynamic quenchers; however, the reverse situation, described by Lehrer in 1976, is worthy of noting at this point. Here, the Stern–Volmer equation has been modified for cases where one dynamic quencher can interact with several fluorophores in different environments. This model has applications in biology where the tryptophans in a protein can be surrounded by amino groups of different polarity and spatial requirements, which result in the different quenching of each of the tryptophans (Lehrer 1976).

2.2. The theory of static fluorescence quenching

The quenching of fluorescence by halide may also occur by a static process, where a non-fluorescent complex is formed and no diffusion processes are involved. In the simplest case

$$\frac{I_0}{I} = 1 + K_S[Q] \quad (17)$$

where K_S is the static quenching constant.

Here the dependence of I_0/I on $[Q]$ is also linear and is very similar to that observed for dynamic quenching except that the quenching constant is now the association constant of the complex. The complexed fluorophores are non-fluorescent and the only observed fluorescence is from the uncomplexed fluorophores (figure 3). Since the uncomplexed fluorophore is unperturbed its lifetime is still τ_0 . Therefore for static quenching $\tau_0/\tau = 1$, whereas for dynamic quenching $\tau_0/\tau = I_0/I$.

Distinguishing between dynamic and static quenching processes can be straightforward, as the dynamic bimolecular rate constant, k_q , increases with temperature, $k_q \propto T/\eta$, equation (6), compared to the decrease in static quenching

constants with temperature, a result of the decrease in stability and subsequent break-up of the non-fluorescent ground state complexes (figure 4). It is also possible to distinguish between these two mechanisms of quenching by simple examination of the absorption spectrum of the system under study. Since collisional quenching only affects the excited state of the fluorophore then there are typically no changes in fluorophore absorption spectra whereas ground state complex formation and subsequent static quenching frequently results in the absorption spectrum being altered.

When both dynamic and static fluorescence quenching occur together then a modified form of the Stern–Volmer equation is used, equation (18), and a steady-state fluorescence plot of I_0/I versus $[Q]$ will usually be upward curving (the equation is second order in $[Q]$, figure 5(A)), and a plot of τ_0/τ should represent only the dynamic quenching component.

$$\frac{I_0}{I} = (1 + K_{SV}[Q])(1 + K_S[Q]). \quad (18)$$

If fluorescence lifetime measurements are unavailable it is possible that equation (18) can be modified to resolve both the static and dynamic components graphically, figure 5(B). The expansion of the parentheses of equation (18) yields

$$\frac{I_0}{I} = 1 + (K_{SV} + K_S)[Q] + K_{SV}K_S[Q]^2 \quad (19)$$

and

$$\frac{I_0}{I} = 1 + K_{APP}[Q] \quad (20)$$

where

$$K_{APP} = \left(\frac{I_0}{I} - 1 \right) \frac{1}{[Q]} = (K_{SV} + K_S) + K_{SV}K_S[Q]. \quad (21)$$

Here K_{APP} is the apparent quenching constant and is typically calculated at each quencher concentration. A plot of K_{APP} versus $[Q]$ gives a straight line with an intercept I of $K_{SV} + K_S$ and a gradient G of $K_{SV}K_S$ (figure 5(B)). The individual values can then be obtained from the two solutions of the resultant quadratic equation, obtained by substitution and rearrangement, equation (22), where additional information such as the temperature or viscosity dependence of the values is used as a basis for assigning them.

$$K_S^2 - K_S I + G = 0. \quad (22)$$

2.2.1. The ‘sphere of action’ static quenching model. Another type of static quenching is often observed at high quencher concentrations due to the existence of an increasing numbers of quencher–fluorophore pairs in which the quencher is close enough to the fluorophore upon excitation to instantly quench its excited state. In solution, this critical distance defines an interaction sphere of volume V . The probability of the quencher being within this volume at the time of excitation depends on both the quencher concentration and the volume. Assuming that the quencher is randomly distributed in solution, the probability of static quenching is given by a Poisson distribution, $e^{-V[Q]}$, and the static quenching mechanism is described by equation (23).

$$\frac{I_0}{I} e^{-V[Q]} = \frac{\tau_0}{\tau}. \quad (23)$$

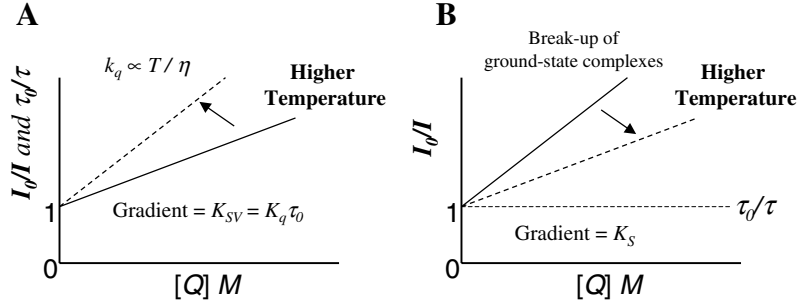


Figure 4. Illustration of the different dependences of fluorescence intensity and lifetime on temperature for dynamic, plot A, and static quenching, plot B. For dynamic quenching $\tau_0/\tau = I_0/I$ and for static quenching $\tau_0/\tau = 1$.

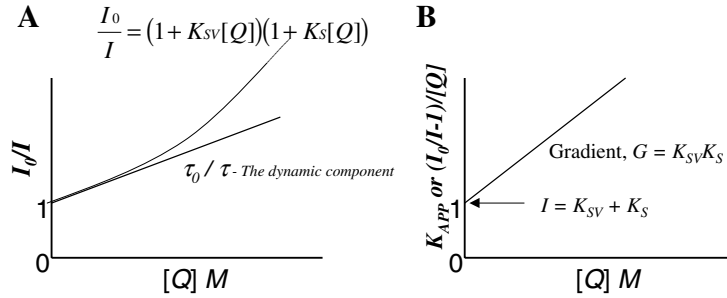


Figure 5. Illustration of dynamic and static quenching for the same population of fluorophores.

It has been shown that the combination of this static quenching mechanism with dynamic quenching, as described by equation (1), results in equation (24) (Laws and Contino 1992),

$$\frac{I_0}{I} = (1 + K_{SV}[Q]) e^{V[Q]} \quad (24)$$

where V must be non-zero since it represents the volume in which quenching occurs without the need for diffusion and must be within a range of values that denotes a radius that is not much larger than the van der Waals radii; a range of $1-3 \text{ M}^{-1}$ yields typical radii ($<10 \text{ \AA}$) for diffusionless interactions (Eftink and Ghiron 1981). Similarly to equation (18), equation (24) typically produces upward curving plots but fortunately the two forms of static quenching may be distinguished as the *sphere of action* static quenching model does not produce changes in the steady-state absorption spectrum. It should be noted that equations (18) and (24) are very similar, especially when $[Q]$ is small. This is because at low $[Q]$, $\exp(V[Q])$ is approximately equal to $1 + V[Q]$, i.e. $1 + x$ is simply the expansion of $\exp(x)$ when x is small.

2.3. Fractional accessibility to quenchers: two fluorophore populations

In the last section we saw how static quenching can lead to positive deviations from Stern–Volmer behaviour. However, it is possible the negative deviations from Stern–Volmer behaviour can occur (curvature towards the x -axis) when two populations of fluorophore are present, one being *accessible to halide* (a) and the other *inaccessible or buried* (b) (figure 6(A)). This fractional accessibility has been observed with the iodide quenching of tryptophan residues (Lehrer 1971) and more recently in three halide sensors which will be described in more detail later (Wyatt *et al* 1987).

The total fluorescence emission intensity in the absence of quencher is given by

$$I_0 = I_0^a + I_0^b \quad (25)$$

where the subscript (0) refers to the fluorescence intensity in the absence of quencher. In the presence of quencher, Q , the intensity of the accessible fraction, I^a , is decreased in the usual Stern–Volmer manner, i.e. equation (1), whereas the buried fraction is unquenched. Therefore the observed fluorescence intensity, I , is given by

$$I = \frac{I_0^a}{1 + K_{SV}^a[Q]} + I_0^b \quad (26)$$

where K_{SV}^a is the Stern–Volmer quenching constant of the accessible fraction. Subtraction of equation (26) from equation (25) gives

$$\Delta I = I_0 - I = I_0^a \left(\frac{K_{SV}^a[Q]}{1 + K_{SV}^a[Q]} \right). \quad (27)$$

Inversion of equation (27) followed by its division into equation (25) gives

$$\frac{I_0}{\Delta I} = \frac{1}{f_a K_{SV}^a[Q]} + \frac{1}{f_a}. \quad (28)$$

Here f_a is the fraction of the initial fluorescence which is accessible to quencher, where

$$f_a = \frac{I_0^a}{I_0^a + I_0^b}. \quad (29)$$

Hence, this modified form of the Stern–Volmer equation allows for K_{SV}^a and f_a to be determined graphically (figure 6(B)).

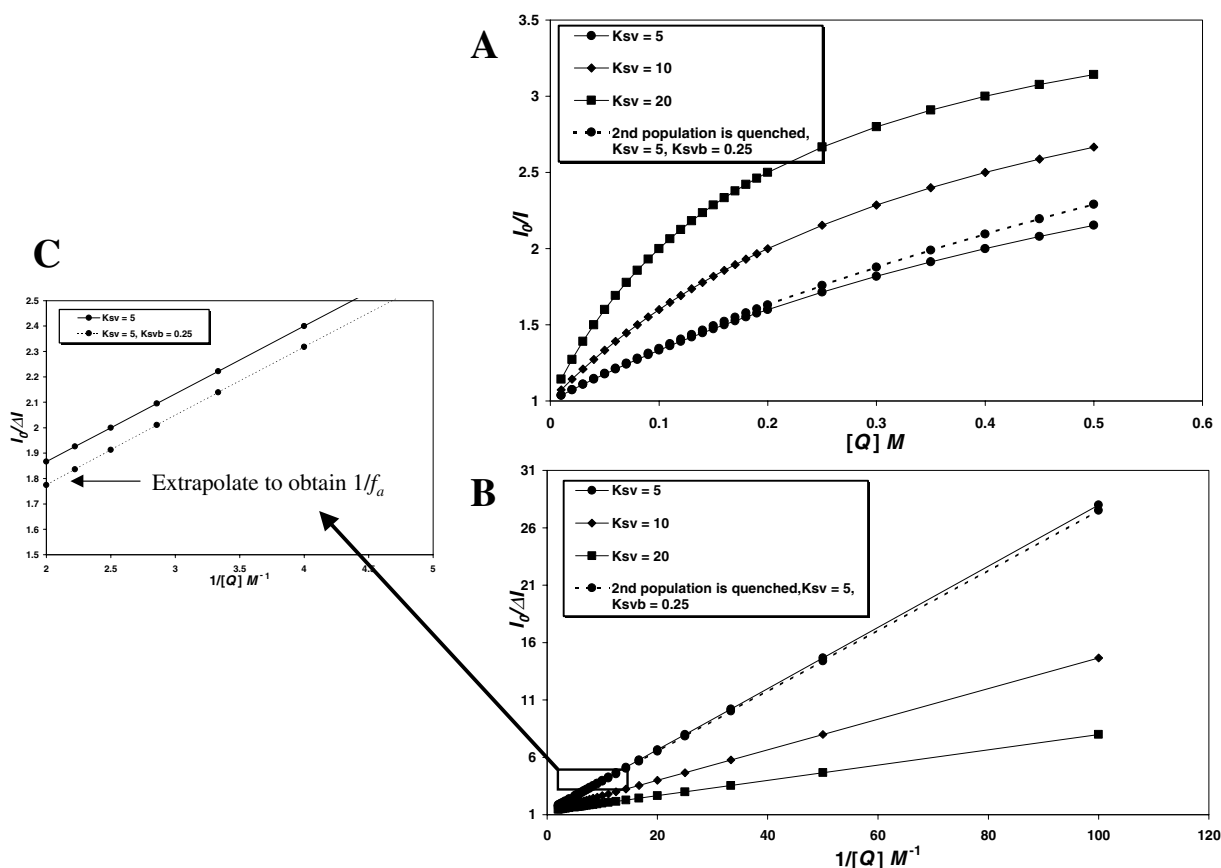


Figure 6. Simulated Stern–Volmer plots (A) and simulated modified Stern–Volmer plots (B) for two populations of fluorophores, where K_{SV}^a has been varied. The intensity of accessible fraction, I_0^a , contributes 75% of the total fluorescence intensity. The dashed lines represent the situation where the 25% inaccessible fraction of fluorescence is quenched with a K_{SV} one-20th that of the accessible fraction, i.e. $K_{SV}^a = 5 M^{-1}$ and $K_{SV}^b = 0.25 M^{-1}$. Plot (C) shows an enlarged region of plot (B). All K_{SV} values have units of M^{-1} .

In these simulated results, $I_0/\Delta I$ against $1/[Q]$ gives the gradient as $1/f_a K_{SV}^a$ and the intercept as $1/f_a$. Interestingly the intercept represents the extrapolation to infinite quencher concentration, i.e. $1/[Q] = 0$. The value of $I_0/(I_0 - I)$ at this quencher concentration therefore represents the fluorescence which is quenched and only the inaccessible buried fluorophore will be fluorescent.

In practice, when using this model to separate the accessible and buried fractions of the total fluorescence, it should be realized that there may be more than two classes of fluorophores present (described in the next section) or the presumed ‘inaccessible’ fraction may in fact be partially accessible to quencher. The author has illustrated this possibility in figure 6, which shows the simulated result if the K_{SV} value for the buried fraction is one-20th of that for the accessible fraction, i.e. a comparison when $K_{SV}^a = 5$ and $K_{SV}^b = 0.25$. For a limited range of quencher concentrations and particular K_{SV} values, this modified Stern–Volmer plot can still appear to be linear. The value of f_a would represent an unrealistic larger value, somewhat larger than that expected for $K_{SV}^b = 0$ (figure 6(C)). Therefore this graphical approach provides a useful but *arbitrary* resolution to two assumed classes of fluorophores.

2.4. Heterogeneously emitting systems

Many fluorophores located in the same system, each with their own distinct K_{SV} values, can also lead to nonlinear Stern–Volmer plots. The situation of finding multiple fluorophores can arise in several ways, even in a chemically pure system. For example, if a protein has more than one tryptophan residue, each one could have a different K_{SV} value due to either a different k_q , τ_0 , or both. It is possible that a polymer can be covalently labelled with *one* halide sensitive fluorophore at a single location but which has different structural conformations in the ground state due to factors such as solubility etc, and therefore several different environments produce different K_{SV} values (Geddes and Douglas 2000). It is also possible that a halide sensitive fluorophore can be immobilized in a support, without covalently binding it, but which also produces many different K_{SV} values due to the simple fact of dye heterogeneity within the support (Zhu *et al* 1990). Such considerations are crucial in understanding the quenching kinetics of immobilized dye halide sensors.

If each species could be spectrally isolated, i.e. would have resolved emission characteristics, then the simple Stern–Volmer expression, the ground state complex model and the sphere of action quenching model (equations (1), (17) and (24) respectively) could be used for analysis. However, for most systems that display this complex behaviour the excitation and/or emission energies are often very similar and

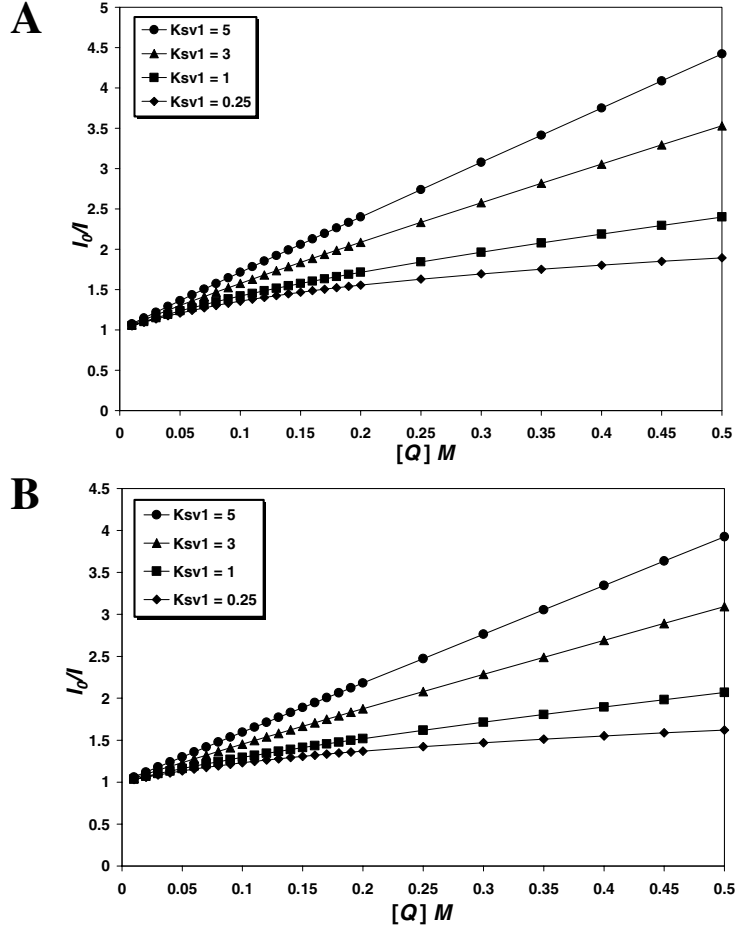


Figure 7. Simulated Stern–Volmer plots for a heterogeneous population of fluorophores undergoing dynamic quenching, where K_{SV1} has been varied. For plot (A) (equation (30)) $K_{SV2} = 10 \text{ M}^{-1}$ and $f_1 = f_2 = 0.5$. For plot (B) $f_1 = 0.6$, $f_2 = 0.3$, $f_3 = 0.1$ and $K_{SV2} = 7 \text{ M}^{-1}$ and $K_{SV3} = 10 \text{ M}^{-1}$.

the measured I_0 and I values, therefore, consist of the weighted sums of the I_0 and I values for each individual species. This means that I_0/I will be a function of $\sum(1 + K_{SV}(i)[Q])$ where i denotes a specific K_{SV} value per species. This is in fact an extension of equation (1) and is similar to the extended Stern–Volmer equation derived in section 2.1.2, where they both assume that the individual species act independently and do not interact with one another. For dynamic quenching then the complete expression for multiple species must weight each element of this summation by the respective fractional intensity, $f(i)$, of each fluorescent species. These $f(i)$ are a function of concentration, quantum yield, extinction and the emission spectrum of each individual fluorescent species. For multiple (n) species undergoing only dynamic quenching,

$$\frac{I_0}{I} = \left[\sum_{i=1}^n \frac{f(i)}{1 + K_{SV}(i)[Q]} \right]^{-1} \quad (30)$$

where by definition $\sum f(i) = 1$.

Figure 7 shows the simulated effects of similar and different K_{SV} values on the degree of curvature of equation (30). We can see the general downward curvature since the initial slope of the intensity ratio is influenced by the largest K_{SV} value. As the concentration of quencher increases, the effect of the smallest K_{SV} terms starts to be seen

and the average K_{SV} will be smaller, resulting in the overall downward curvature. We can also see that when two K_{SV} values are similar the expression appears linear as compared to the downward curvature when the K_{SV} values are significantly different. Figure 7(B) shows the more complex simulated results obtained for three populations of fluorophores, each with different K_{SV} values and fractional intensity.

It is also possible that a heterogeneous population of dynamically quenched fluorophores can undergo static quenching by either of the two models described in sections 2.2 and 2.2.1. For ground state complex formation, the measured fluorescence intensity ratio, I_0/I , can be described by

$$\frac{I_0}{I} = \left[\sum_{i=1}^n \frac{f(i)}{\{1 + K_{SV}(i)[Q]\}\{1 + K_S(i)[Q]\}} \right]^{-1} \quad (31)$$

where K_S is the static quenching constant (figure 8(A)). This expression typically causes upward curvature, even when the K_{SV} values are significantly different.

Similarly for the sphere of action static quenching model, if we introduce an $e^{V[Q]}$ term for each emitting species, i.e. $e^{V(i)[Q]}$, then under these conditions the fluorescence intensity ratio, I_0/I , can be described by

$$\frac{I_0}{I} = \left[\sum_{i=1}^n \frac{f(i)}{\{1 + K_{SV}(i)[Q]\} e^{V(i)[Q]}} \right]^{-1} \quad (32)$$

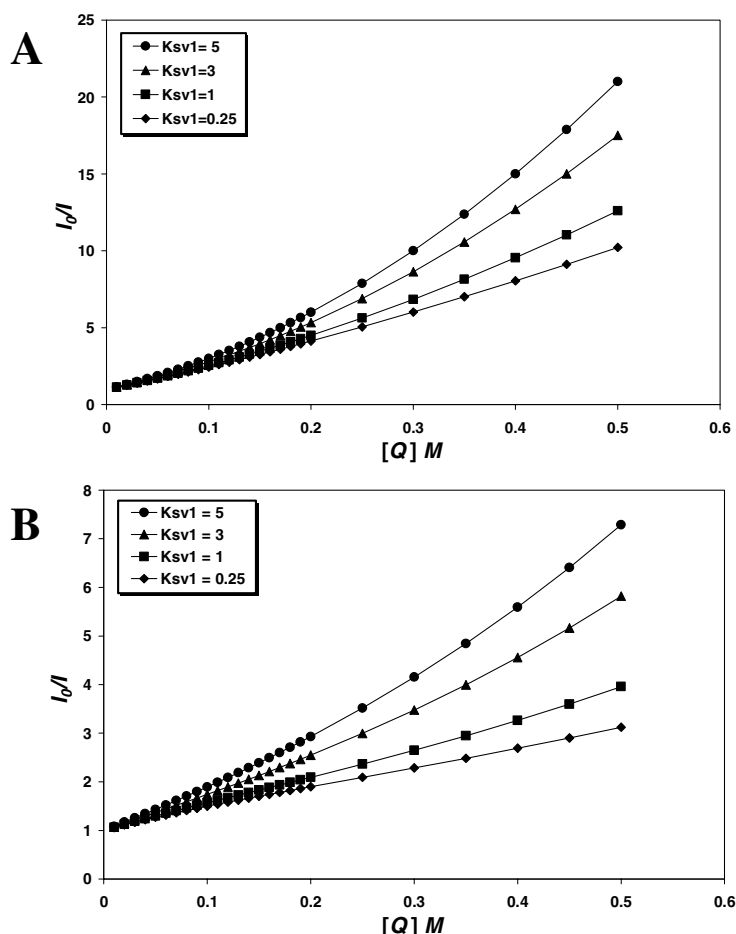


Figure 8. Simulated Stern–Volmer plots for a heterogeneous population of fluorophores undergoing (A) dynamic and ground state complex formation static quenching and (B) dynamic and the sphere of action static quenching, where K_{SV1} has been varied. For plot (A) (equation (31)) $K_{SV2} = 5 \text{ M}^{-1}$, $K_{S1} = K_{S2} = 10 \text{ M}^{-1}$ and $f_1 = f_2 = 0.5$. For plot (B) (equation (32)) $K_{SV2} = 10 \text{ M}^{-1}$, $V_1 = V_2 = 1 \text{ M}^{-1}$ and $f_1 = f_2 = 0.5$.

The curvature of any data described by this quenching mechanism depends on the specific values of $f(i)$, $K_{SV}(i)$ and $V(i)$ (figure 8(B)). We can clearly see that the addition of the static quenching component can counteract any downward curvature due to different K_{SV} values and causes either linear behaviour or upward curvature. Moreover, a close inspection of the simulated data for $K_{SV1} = 1 \text{ M}^{-1}$ shows that this curve is somewhat complex, where upward curvature occurs after a small amount of downward curvature.

2.5. Fluorescence resonance energy transfer (FRET)

Another important quenching process which has been used to sense halide is fluorescence resonance energy transfer. FRET is the transfer of the excited state energy from the initially excited donor, D, to an acceptor, A, which is typically non-fluorescent (figure 1(A)). The donor emission spectrum typically overlaps with the absorption spectrum of the acceptor (figure 9). As will be seen later (section 3.3), for halide sensing, the acceptor molecule is not a solvated halide ion as these are colourless, but instead the sensing mechanism involves monitoring either the donor or acceptor fluorescence intensity or lifetime during FRET, in the presence and absence of halide.

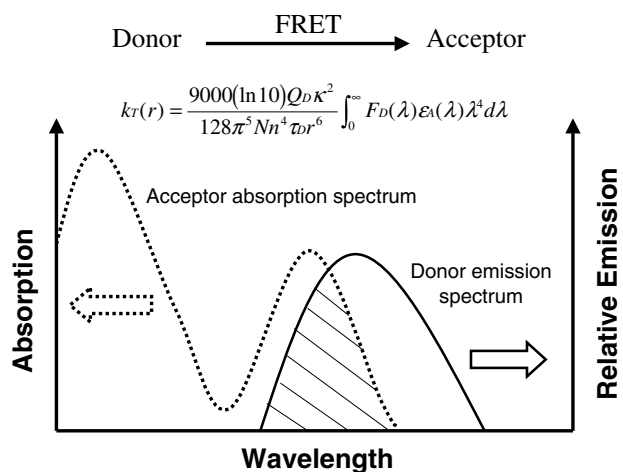


Figure 9. The overlap of donor emission and acceptor absorption spectra for FRET.

FRET occurs without the emission and transfer of a photon but is the result of long-range dipole–dipole interactions between the donor and acceptor. The donor fluorophore may be thought of as an oscillating dipole that can exchange energy with an acceptor dipole of similar resonance frequency

(Cheung 1991, Lakowicz 1999). One important characteristic of FRET is that it occurs over distances that are comparable to the dimensions of biological molecules and has therefore been used extensively as a 'molecular ruler' to study processes as desperate as protein sizing and folding (Steinberg 1971, Stryer 1978).

The rate of energy transfer from a donor to an acceptor, k_T , is given by

$$k_T = \frac{1}{\tau_D} \left(\frac{R_0}{r} \right)^6 \quad (33)$$

where τ_D is the decay time of the donor in the absence of the acceptor, R_0 is the Förster distance (the distance at which the efficiency of FRET is 50%) and r is the donor to acceptor distance. As can be seen from equation (33) the rate of FRET depends strongly on distance, being inversely proportional to r^6 . It is often convenient to write equation (33) in terms of the Förster distance R_0 , at which the transfer rate $k_T(r)$ is equal to the decay rate of the donor in the absence of acceptor (τ_D^{-1}). At this distance, one half of the donor molecules decay by energy transfer and one half decay by the usual radiative and non-radiative processes (equation (34)).

$$R_0^6 = \frac{9000(\ln 10)\kappa^2 Q_D}{128\pi^5 N n^4} \int_0^\infty F_D(\lambda) \varepsilon_A(\lambda) \lambda^4 d\lambda \quad (34)$$

where Q_D is the quantum yield of the donor in the absence of acceptor, n is the refractive index of the medium, N is Avogadro's number, $F_D(\lambda)$ is the corrected fluorescence intensity of the donor in the wavelength range λ to $\lambda + \Delta\lambda$, with the total intensity (area under the curve) normalized to unity, $\varepsilon_A(\lambda)$ is the extinction coefficient of the acceptor at λ and κ^2 is a factor describing the relative orientation of the transition dipoles of the donor and acceptor. This equation allows the Förster distance to be calculated from the spectral properties of the donor and acceptor and the donor quantum yield. The theory of FRET is moderately complex and therefore the author directs readers to a very good overview containing the final derived equations of FRET (Lakowicz 1999) and a review with a more physical explanation of FRET (Clegg 1996).

2.6. Charge effects on quenching

The extent of quenching of a fluorophore can be affected by its surrounding environment (Lakowicz 1999). It has been shown by Ando and Asai that the comparison between charged (I^-) and neutral (acrylamide) quenchers can reveal the sign of the electrostatic potential near a fluorophore attached to a macromolecule (Ando and Asai 1980). By varying the ionic strength they show that one can determine the number of adjacent charges and their distance from a fluorophore. The apparent quenching rate constant, k_q^* , for a charged quencher will be

$$\log k_q^* = \log k_q + 0.434 \frac{Z_0 Z_m e_0^2}{k_b T R_0^*} \left(1 - \frac{1}{D} \right) + C Z_0 Z_M \sqrt{\mu} \quad (35)$$

where k_q is the rate constant in the absence of electrostatic effects, Z_0 and Z_m are the charges on the quencher and macromolecule near the fluorophore respectively, e_0 is the elementary charge, D is the dielectric constant, R_0^* is the

distance of closest approach of the quencher and fluorophore, C is a constant (1.02 for aqueous solutions at 25 °C) and μ is ionic strength. Hence, determining k_q^* , for a quencher of charge Z_0 , as a function of ionic strength, one can determine Z_m , the charge near the fluorophore.

The electrostatic effects of quenching are typically only applicable to charged quenchers such as the halides and are absent for neutral quenchers such as oxygen and acrylamide and therefore can be minimized by working at a high and fixed ionic strength.

2.7. The effects of dissolved oxygen

Almost all fluorophores are quenched by molecular oxygen (Kautsky 1939, Ware 1962, Lakowicz and Weber 1973) and hence for aqueous or gaseous halide sensing it is necessary to remove oxygen. If halide sensing occurs in the presence of oxygen then the measured fluorescence intensity or lifetime will typically be unreliable and the ratio I_0/I may be described by the 'extended Stern–Volmer' equation, section 2.1.2. For systems where dissolved oxygen cannot be removed, e.g. the *in situ* measurements of halide in blood, then the extended Stern–Volmer equation can become ideal (under certain conditions) for describing the quenching kinetics.

The mechanism by which oxygen quenches fluorescence has been the subject of debate for some time but the most likely mechanism is that the paramagnetic oxygen causes the fluorophore to undergo intersystem crossing to the triplet state which is then quenched by other deactivation processes (Lakowicz 1999). Fluorophores with lifetimes under ≈ 5 ns are typically not quenched by dissolved oxygen, although many authors have reported negligible effects for probes with lifetimes up to ≈ 20 ns. This value, whilst just approximate, can be quite simply explained in terms of diffusion. The

root-mean-square distance, $\sqrt{(\Delta x^2)}$, over which a quencher can diffuse during the unquenched excited state lifetime of a fluorophore, τ_0 , is given by $\sqrt{(\Delta x^2)} = \sqrt{(2D\tau_0)}$, where D is the diffusion coefficient. Given that an oxygen molecule at 25 °C has a diffusion coefficient of $2.5 \times 10^{-5} \text{ cm}^2 \text{ s}^{-1}$ (Lakowicz 1999), then during a typical lifetime of 5 ns the oxygen molecule can diffuse 50 Å. If the lifetime is longer, diffusion over larger distances is observed and hence there is a greater chance of quenching the excited state of the fluorophore. It is in essence, this diffusion aspect of oxygen during the lifetime of long-lived probes, which enables oxygen to be sensed by fluorescence or phosphorescence collisional quenching. In fact to obtain sensitivity at low concentrations of oxygen then fluorophores which have *very long* lifetimes in the absence of oxygen are chosen, such as transition-metal complexes (Bacon and Demas 1987, Wolfbeis 1991, Demas and DeGraff 1994, Mills and Williams 1997). For oxygen sensors then these complexes are typically dissolved in silicone in which oxygen is very soluble and freely diffusing. The silicone also serves as a barrier to interfering molecules where the silicone is impermeable to most polar species. Since there are typically no other species in air which can act as collisional quenchers, these types of sensor show excellent selectivity to oxygen (Cox and Dunn 1985, Charlesworth 1994, Xu *et al* 1996).

Over the past 10 years a significant amount of effort has been applied to unravelling the quenching kinetics of immobilized transition-metal complexes by oxygen and as a result many quenching models have been thoroughly investigated. This has provided a wealth of literature and subsequently a framework on which future immobilized dye halide sensors will probably be based (Carraway *et al* 1991a, b, Mills 1998a, b, 1999a, b).

3. Optical halide sensing using fluorescence quenching: applications

The past two decades have seen the rapid growth of fluorescence spectroscopy. This has been partly due to the development of new light sources, i.e. the transformation from nanosecond flash lamps to picosecond dye lasers or femtosecond Ti:sapphire lasers, as well as the realization that much more information is contained *in* and can be extracted *from* a fluorescence decay. The expansion of fluorescence has also been helped by the race for the humane genome, where prior to 1985, most DNA sequencing was performed using radioactive labels (Lakowicz 1999). Since that time, sequencing has been accomplished almost exclusively using new carefully designed fluorescent probes. It has been the development of new fluorescent probes for many different fluorescence based disciplines that has inevitably led to their application *in*, and therefore the growth *of*, optical halide sensing using fluorescence quenching.

3.1. Halide sensitive fluorophores

It is almost a case of historical coincidence when we realize that the first solution quenching studies performed by Stokes in 1869 used the quinine molecule (Stokes 1869), and that one of the first halide sensors, which involved the immobilization of a fluorophore on a glass substrate reported over 100 years later (Urbano *et al* 1984), also used a quinine derivative, namely 6-methoxy-N-(3-sulphopropyl)quinolinium, better known today as SPQ in the research literature. It was perhaps using the hint that quinine, which contains a quinolinium ring, was sensitive to halide that both SPQ and many other new compounds containing this ring have subsequently been made (Wolfbeis and Urbano 1982, Krapf *et al* 1988, Geddes *et al* 1999a, 2001a, b). In one of the very few studies of its kind for halide sensing, Krapf *et al* have studied the structure–activity relationships for 6-methoxyquinoline, 6MQ, and similar nuclei and have shown that the SPQ molecule offers both good water solubility and halide sensitivity (Krapf *et al* 1988). Table 2, shows a few quinolinium type fluorophores that have been used for halide sensing along with their corresponding Stern–Volmer constants for aqueous halide.

It is interesting to compare the K_{SV} values for some of the dyes in table 2. A comparison of dyes A and B shows that the length of the sulphoalkyl chain has an effect on the magnitude of the K_{SV} values as does a methyl or methoxy substituent in the 6-position, i.e. a comparison of dyes A and D respectively. Recently Geddes *et al* have also investigated this chain length dependence for 6MQ using carboxylic acid chains, and have also shown a decrease in K_{SV} values, for longer alkyl chains substituted on the quaternary nitrogen centre (Geddes *et al*

1999a, b). In addition, Geddes *et al* have also investigated the effect of counter-ion on halide sensitivity, dyes E and F, and show a significant reduction in K_{SV} values for probes with the larger tetraphenyl boron counter-ion. The authors suggest the reduction may be due to steric hindrance of the quencher by the counter-ion (dynamic quenching is a diffusion controlled process) or even may be due to the poor aqueous solubility of dye F (Geddes *et al* 1999a). A comparison of dyes G and H shows again the effect that the counter-ion has on the magnitude of halide K_{SV} values. Here it is likely that a static quenching process is responsible for this effect, given that the dye and counter-ion will probably exist as a solvated ion pair. Recently it has been suggested that the quenching of quinolinium fluorescence by anions in water involves a charge transfer process (Jayaraman and Verkman 2000). As a result of their findings, Jayaraman and Verkman envisage being able to design improved chloride sensitive indicators in the future from a better fundamental understanding of the structural relationships with respect to quenching.

One particular useful property of dyes based on 6MQ or 6MeQ is the large Stokes shift in the fluorescence emission spectrum with respect to the excitation, in some cases over 100 nm, indicating a significant energy gap between the ground and first excited singlet states. In practise the ease of discrimination between these two states allows for use of ‘cut-off’ filters rather than interference filters with only very little loss in excitation and emission energy. This is often an important consideration in immobilized dye type sensors operating at low signal-to-noise ratios (Geddes 2001) as well as minimizing any potential dye–dye non-radiative energy transfer processes. Table 3 shows absorption and emission wavelength maxima for some dyes used in aqueous halide sensing. It is interesting to see from table 3 the recent identification of long-wavelength halide sensitive indicators such as LZQ (Jayaraman *et al* 1999b), which has benefits from not requiring ultraviolet excitation such as the reduced scattering of the excitation light, λ^{-4} dependence, reduced sample degradation and a better compatibility with low-cost laser diode excitation sources.

Other nuclei which have been particularly useful in halide sensing include acridine, harmane³ and the rhodamines, tables 4, 5 and 6 respectively.

One notable feature of table 4 is the magnitude of some of the K_{SV} values as compared to those shown in the other tables. We can see that lucigenin (dye C) is highly chloride sensitive, and likewise dye B is one of the most sensitive probes reported for aqueous iodide. The K_{SV} values for dye C (table 2) are also relatively large, but these data were obtained in a non-aqueous medium and, as suggested, the large K_{SV} values can be attributed to the increased fluorescence lifetime of the probe in methanol as compared to water (Jiwan and Soumillion 1997). One other noticeable feature for all the probes shown in tables 2 and 4–6 is the greater sensitivity of the fluorescent probes to iodide as compared to bromide and chloride.

3.1.1. Halide selectivity. Of the three halides readily sensed by fluorescence quenching methods, it is the chloride ion sensitivity that is generally remarked upon by

³ Harmane (1-methyl-9H-pyrido[3,4-b]indole), is sometimes also referred to as aribine or harman in the research literature.

Table 2. Quinolinium type molecules that have been used/considered for halide sensing and their corresponding K_{SV} values (M^{-1}).

	Fluorophore	Fluorophore ^a	Halide	Solvent	Solution K_{sv}	Supported K_{sv}	Matrix	Ref.
A		SPQ 6-methoxy-N-(3-sulphopropyl)quinolinium	Cl ⁻ Br ⁻ I ⁻	H ₂ O pH7.4	118 175 276	— — —	— — —	Krapf <i>et al</i> 1988
B		6-methoxy-N-(4-sulphobutyl)quinolinium	Cl ⁻ Br ⁻ I ⁻	H ₂ O pH7.4	78 154 233	— — —	— — —	Krapf <i>et al</i> 1988
C		N-dodecyl-6-methoxyquinolinium iodide	Cl ⁻ Br ⁻ I ⁻	MeOH	536 583 850	K_{SV1} 0.15 ^b K_{SV2} 25.6 0.46 ^b 64.3 2.96 ^b 281	Sol-gel	Jiwan and Soumillion 1997
D		6-methyl-N-(3-sulphopropyl)quinolinium	Cl ⁻ Br ⁻ I ⁻	H ₂ O pH7.4	83 123 171	— — —	— — —	Krapf <i>et al</i> 1988
E		6-methoxy-N-(8-octanoic acid)quinolinium bromide	Cl ⁻ Br ⁻ I ⁻	H ₂ O pH10	52 225 634	16 ^c 64 ^c 192 ^c	Nq 11 ^d 66 ^d	Organic polymer Geddes and Douglas 2000
F		6-methoxy-N-(8-octanoic acid)quinolinium tetraphenyl borate	Cl ⁻ Br ⁻ I ⁻	H ₂ O/ EtOH pH10	20 70 218	Nq 10 ^c 47 ^c	Nq 5 ^d 29 ^d	Organic polymer Geddes and Douglas 2000
G		6-methyl-N-(methyl)quinolinium bromide	Cl ⁻ Br ⁻ I ⁻	H ₂ O pH7.0	255 421 645	— — —	— — —	Geddes <i>et al</i> 2001a
H		6-methyl-N-(methyl)quinolinium iodide	Cl ⁻ Br ⁻ I ⁻	H ₂ O pH7.0	162 266 370	— — —	— — —	Geddes <i>et al</i> 2001a

'—' indicates fluorophore was not supported in a matrix.

Nq indicates no detectable quenching.

^a Formulae are as presented in the respective references.

^b To obtain the Stern–Volmer constants, the data have been fitted to a Stern–Volmer function which describes the heterogeneous quenching of dye in the sol-gel matrix, i.e. equation (30), section 2.4: $I/I_0 = f_1/(1 + K_{SV1}[Q]) + f_2/(1 + K_{SV2}[Q])$, where f_1 and f_2 are the relative weighting factors.

^c Unbound fluorophore, fluorophore mixed within the support but not covalently bound.

^d Fluorophore covalently bound to copolymer.

most workers. This is not because bromide and iodide are not as environmentally or physiologically important, quite the contrary as discussed in section 1, but because for the halides the quenching of fluorescence is not a selective process, and any fluorophore quenched by chloride is also quenched by bromide to a greater extent and also by iodide to an even greater extent. Therefore for dynamic quenching the sensitivity of fluorophores to halide is in the order $I^- > Br^- > Cl^-$. The explanation to this effect lies in the fact that the efficiency of intersystem crossing to the excited triplet state, promoted by spin-orbit coupling of the excited singlet fluorophore and

halide upon contact, depends on the mass of the quencher atom, hence the expression 'heavy-atom effect' is sometimes used (figure 1) (Turro 1991).

Since fluorescence quenching is therefore not a selective process (this is generally true, although some proteins have specific halide binding sites, Wachter *et al* 2000, Jayaraman *et al* 2000), then halide quenching measurements are also subject to other heavy-atom and diffusional quenching based interferences (Fabrizzi *et al* 1996). For example, it is reported that lucigenin, MAA, MACA and MAMC (table 4) are also sensitive to the SCN^- anion with relatively large K_{SV} values

Table 3. Absorption, λ_{abs} max, and emission, λ_{em} max, wavelength maxima for some dyes used in aqueous halide sensing.

Fluorophore	Solvent	λ_{abs} max (nm)	λ_{em} max (nm)	Ref.
SPQ—dye A, table 2	H ₂ O/pH 7.4	318	442	Krapf <i>et al</i> 1988
Dye E, table 2	H ₂ O/ pH 10	360	460	Geddes and Douglas 2000
Dye F, table 2	H ₂ O/ EtOH, pH 10	360	460	Geddes and Douglas 2000
Dye H, table 2	H ₂ O/ pH 7.0	320	420	Geddes <i>et al</i> 2001a
LZQ—see glossary of acronyms	H ₂ O/pH 5–8	400–470	490–560	Jayaraman <i>et al</i> 1999b
SPA—dye A, table 4	H ₂ O/pH 10	360	490	Geddes 2000a
Lucigenin—dye C, table 4	H ₂ O/pH 7.2	368/455	506	Biwersi <i>et al</i> 1994
MAA—dye D, table 4	H ₂ O/pH 7.2	400/422	457/480	Biwersi <i>et al</i> 1994
MACA—dye E, table 4	H ₂ O/pH 7.2	364/422	500	Biwersi <i>et al</i> 1994
MAMC—dye F, table 4	H ₂ O/pH 7.2	366/424	517	Biwersi <i>et al</i> 1994
SPI—dye B, table 5	H ₂ O/pH 10	390	410, 460	Geddes 2000b
Dye C, table 5	H ₂ O/pH 10	390	460	Geddes and Douglas 2000
RhB, dye A, table 6	H ₂ O/pH 10	550	580	Geddes and Douglas 2000
R6G, dye B, table 6	H ₂ O/pH 10	530	550	Geddes and Douglas 2000

of 590, 211, 480 and 283 M⁻¹ respectively (Biwersi *et al* 1994). Geddes and Douglas have also reported the interference of the sulphite anion on various quinolinium, indolium and rhodamine based optical halide sensors (Geddes and Douglas 2000). Dissolved oxygen is also a problem in halide sensing measurements, as discussed in section 2.7, and therefore for halide sensing, probes with lifetimes typically less than ≈ 20 ns should be used. Of course a 200 ns transition-metal-ion complex used for oxygen sensing will probably also be highly sensitive towards halide, but will inevitably be sensitive to most other aqueous ions and dissolved gases as well. If interference concentrations are known and dissolved oxygen can readily be removed, or corrected for, then ‘long-lived’ fluorescent or phosphorescent probes can be used. However, in many halide sensing applications it is not practical to remove oxygen and therefore short-lived fluorescent probes, which are unperturbed by oxygen, have to be used. It is this upper limit of probe fluorescence lifetime (≈ 20 ns) that influences the magnitude of K_{SV} values, i.e. $K_{SV} = k_q\tau_0$, and therefore the workable halide concentration range for fluorescence quenching based optical halide sensors.

3.1.2. The magnitude of K_{SV} : signal-to-noise ratio considerations. It is often the case for new probes reported in the research literature that authors focus on the upper limits of sensitivity (lowest halide concentration) that their probes can detect. However, whilst for certain circumstances this is appropriate, it is often the case that it is the ‘dynamic concentration range’ over which a probes measurements remain reliable, rather than the ultimate halide concentration detectable, that should be the focus. One can illustrate this point by considering the dynamic quenching of dye E (table 2) and lucigenin, dye C (table 4) by aqueous chloride. Here both probes have reported Cl⁻ K_{SV} values of 52 and 390 M⁻¹ respectively. Under the same conditions and for a chloride concentration of 0.126 M, then for lucigenin, 2% of the initial fluorescence intensity is observed, i.e. I in equation (1), as compared to 13.2% for dye E. Similarly, for a chloride concentration of 0.000 65 M then 79.8% and 96.7% of the initial fluorescence intensity is observed for lucigenin and dye E respectively. Therefore we can see from these values that the halide concentration where the fluorescence intensity change is great enough to be measured (i.e. at low halide

concentrations), and where the quenched intensity is actually large enough to be measured through the instrumental/system noise (i.e. at high quencher concentrations), depends on the magnitude of the probe’s K_{SV} value. Therefore for quenching studies, probes should be chosen that give an appreciable change in fluorescence signal that is within the capabilities of the instrumentation. Whilst this is true for steady-state (quantitative intensity) measurements, for lifetime based measurements, which do not depend on total fluorescence intensity, then the only requirement is that the signal is large enough to be measured in a reasonable time-span (see section 3.4.2).

3.2. Solution halide sensing

The popularity of solution fluorescence quenching experiments is evident by the vast number of articles in the research literature (Wolfbeis and Hochmuth 1984, Andrews-Wilberforce and Patonay 1989, Tucker and Acree 1995, Martin and Narayanaswamy 1997), to name a few. This popularity is due to a few factors such as the relative ease with which quenching experiments can be performed, the sensitivity that fluorescence has to offer and the wealth of information that can be obtained in addition to quantitative halide determinations, such as protein or polymer conformational/structural information as well as physiological information, such as halide transport mechanisms (Eftink and Ghiron 1981). Illsley and Verkman have used the SPQ molecule (dye A—table 2) to monitor chloride transport across cell membranes (Illsley and Verkman 1987). Erythrocyte ghosts, the membranes from red blood cells after removal of the intercellular contents, were loaded with both 100 mM Cl⁻ and SPQ. SPQ is readily quenched by aqueous chloride with a greater than 50% decrease in fluorescence intensity at 10 mM chloride and a rapid response of <1 ms (Illsley and Verkman 1987). When the ghosts were diluted into a non-quenching 66 mM K₂SO₄ solution, the intensity of SPQ fluorescence increased owing to the efflux of the chloride. However, by introducing dihydro-4,4′-diisothiocyanostilbene-2,2′-disulphonic acid (H₂DIDS), an inhibitor for anion transport, the chloride transport could be blocked (figure 10). Hence, fluorescence quenching can be used to study halide transport across cells. Similar uses of SPQ in physiology

Table 4. Fluorophores based on the acridine nucleus that have been used/considered for halide sensing and their corresponding K_{SV} values (M^{-1}).

	Fluorophore	Fluorophore ^a	Halide	Solvent	Solution K_{sv}	Supported K_{sv}	Matrix	Ref.
A		SPA N-(sulphopropyl) acridinium	Cl ⁻ Br ⁻ I ⁻	H ₂ O pH10	1 58 374	Nq ^b 5 ^b 196 ^b	Organic polymer	Geddes 2000a
B		3-(10- methylacridinium- 9-yl) propionic acid tetrafluoroboron	Cl ⁻ Br ⁻ I ⁻	H ₂ O pH10	1 47 762	Nq ^b 10 ^b 230 ^b	Organic polymer	Geddes 2000a
C		Lucigenin N,N'-dimethyl-9,9'- bisacridinium	Cl ⁻ Br ⁻ I ⁻	H ₂ O pH7.2	390 585 750	— — —	— — —	Biwersi <i>et al</i> 1994
D		MAA N-methyl-9- aminoacridinium	Cl ⁻ Br ⁻ I ⁻	H ₂ O pH7.2	2 4 253	— — —	— — —	Biwersi <i>et al</i> 1994
E		MACA 10-methylacridinium- 9-carboxamide	Cl ⁻ Br ⁻ I ⁻	H ₂ O pH7.2	225 480 550	— — —	— — —	Biwersi <i>et al</i> 1994
F		MAMC N-methylacridinium- 9-methylcarboxylate	Cl ⁻ Br ⁻ I ⁻	H ₂ O pH7.2	160 250 267	— — —	— — —	Biwersi <i>et al</i> 1994

— indicates fluorophore was not supported in a matrix.

Nq indicates no detectable quenching.

^a Formulae are as presented in the respective references.

^b Unbound fluorophore, fluorophore mixed within the support but not covalently bound.

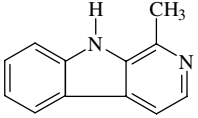
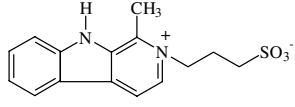
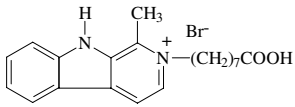
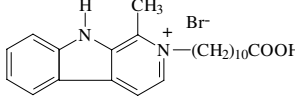
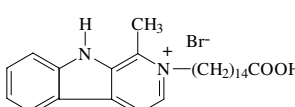
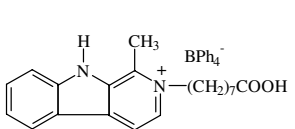
have also been reported (Dwyer and Farley 1991, Greco and Solomon 1997, Pilas and Durack 1997, Srinivas *et al* 1998, Jayaraman *et al* 1999a).

One particular analytical benefit of solution halide sensing using fluorescence quenching is that measurements can be performed on very small sample volumes. Recently, Garcia *et al* have used SPQ to determine chloride concentrations in nanolitre aqueous samples (Garcia *et al* 1999). Their method, which uses an 'ultramicro-fluorometer', in essence a very small sample volume fluorometer, is fairly specific for chloride, although bromide and iodide will interfere. Garcia *et al* report a resolution of 1 mM between 5 and 50 mM and 2.6 mM between 50 and 200 mM chloride. Advantages of their technique are that samples can be measured every four minutes and the ability

to measure Cl⁻ does not vary with pH within the physiological range.

3.2.1. Halide sensing using green and yellow fluorescent proteins. Recently we have seen the introduction of the green fluorescent protein, GFP, to our arsenal of halide sensitive probes. The GFP, originally isolated from the bioluminescent jellyfish *Aequorea victoria*, contains a highly fluorescent chromophore within a constrained and protected region of the protein. This chromophore, which forms spontaneously, is formed by the folding of polypeptide chain within the GFP without the need for enzymatic synthesis (Chalfie *et al* 1994). As a result, the gene for GFP can be inserted into cells to obtain proteins which have attached GFP. A wide variety of

Table 5. Fluorophores based on the harmane nucleus that have been used/considered for halide sensing and their corresponding K_{SV} values (M^{-1}).

	Fluorophore	Fluorophore ^a	Halide	Solvent	Solution K_{sv}	Supported K_{sv}	Matrix	Ref.	
A		Harmane 1-methyl-9H-pyrido[3,4-b]indole	Cl ⁻ Br ⁻ I ⁻	—	—	Nq ^b 22.4 ^b 554 ^b	Cellulose	Zhu <i>et al</i> 1990	
B		SPI 1-methyl-2-(sulphonatopropyl)-9H-pyrido[3,4-b]indolium	Cl ⁻ Br ⁻ I ⁻	H ₂ O pH10	Nq 3 204	Nq ^b 2 ^b 112 ^b	Organic polymer	Geddes 2000b	
C		1-methyl-2-(8-octanoic acid)-9H-pyrido[3,4-b]indolium bromide	Cl ⁻ Br ⁻ I ⁻	H ₂ O pH10	Nq 3 191	Nq ^b 2 15	Nq ^c 2 ^c 7 ^c	Organic polymer	Geddes and Douglas 2000
D		1-methyl-2-(11-undecanoic acid)-9H-pyrido[3,4-b]indolium bromide	Cl ⁻ Br ⁻ I ⁻	H ₂ O pH10	Nq 5 198	Nq ^b 2 15	Nq ^c 2 ^c Nq ^c Nq ^c	Organic polymer	Geddes and Douglas 2000
E		1-methyl-2-(15-pentadecanoic acid)-9H-pyrido[3,4-b]indolium bromide	Cl ⁻ Br ⁻ I ⁻	H ₂ O pH10	Nq 3 192	Nq ^b 2 14	Nq ^c 2 ^c Nq ^c Nq ^c	Organic polymer	Geddes and Douglas 2000
F		1-methyl-2-(8-octanoic acid)-9H-pyrido[3,4-b]indolium tetraphenyl boron	Cl ⁻ Br ⁻ I ⁻	EtOH H ₂ O pH10	Nq 1 139	Nq ^b Nq ^b 8	Nq ^c Nq ^c 1	Organic polymer	Geddes and Douglas 2000

— indicates no data available in reference.

Nq indicates no detectable quenching.

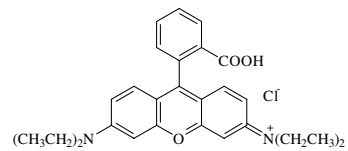
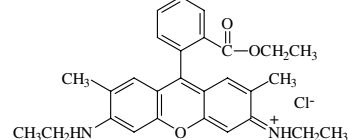
^a Formulae are as presented in the respective references.

^b Unbound fluorophore, fluorophore mixed within the support but not covalently bound.

^c Fluorophore covalently bound.

Harmane is sometimes also referred to as harman or aribine in the research literature.

Table 6. Rhodamine fluorophores that have been used/considered for halide sensing and their corresponding K_{SV} values (M^{-1}).

	Fluorophore	Fluorophore ^a	Halide	Solvent	Solution K_{sv}	Supported K_{sv}	Matrix	Ref.	
A		RhB Rhodamine B	Cl ⁻ Br ⁻ I ⁻	H ₂ O pH10	Nq Nq 5	Nq ^b Nq ^b 1	Nq ^c Nq ^c 1	Organic polymer	Geddes and Douglas 2000
B		R6G Rhodamine 6G	Cl ⁻ Br ⁻ I ⁻	H ₂ O pH10	Nq Nq 24	Nq ^b Nq ^b 4 ^b		Organic polymer	Geddes and Douglas 2000

Nq indicates no detectable quenching.

^a Formulae are as presented in the respective references.

^b Unbound fluorophore, fluorophore mixed within the support but not covalently bound.

^c Fluorophore covalently bound.

different GFP variants have been constructed using genetic engineering techniques and a number of mutations in and around the chromophore have profound effects on the GFP's optical properties. The GFP typically shows time-dependent changes in its spectrum upon excitation at 380 nm, but to

a lesser extent at 475 nm. Mutants are known to display longer wavelength absorption and emission spectra, which also display less dependence on excitation (Heim and Tsien 1996). (For recent reviews on GFPs see Tsien 1998, Palm and Wlodawer 1999).

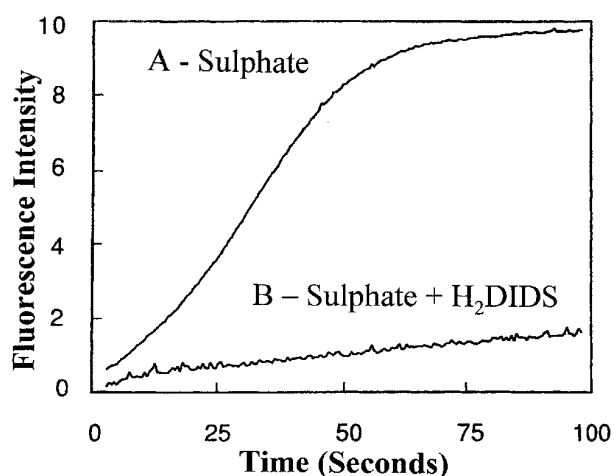


Figure 10. Fluorescence intensity (arb. units) of SPQ in erythrocyte ghosts as a function of time, showing (A) the efflux of chloride from the ghosts into the sulphate containing buffer and (B) the inhibited chloride transport in the presence of the anion-transport inhibitor, H₂DIDS, also in the sulphate containing buffer. Revised and reprinted with permission from Illsley and Verkman 1987, copyright © 1987, American Chemical Society.

The applications for GFPs are rapidly growing (Sullivan and Kay 1999), where one recent biosensor application has involved the use of different colored GFPs for FRET, to monitor calcium concentrations (Miyawaki *et al* 1999). A GFP variant, the yellow fluorescent protein (YFP) is currently attracting a lot of attention in the research literature because the YFP chromophore pK_a shows a strong dependence on the concentration of halide ions (Wachter and Remington 1999), and increases in pK_a from about 5.2 to 7.0 in the presence of 140 mM NaCl (Elsiger *et al* 1999). The sensitivity of these YFPs towards halide results from the pH dependent ground state-binding of halide near the chromophore, which, it has been suggested, alters the ionization constant and subsequently the fluorescence emission spectrum (Jayaraman *et al* 2000). For this sensing mechanism there is no evidence for halide collisional quenching, and the halides act like ligands affecting the chromophores charge state with a stronger level of interaction at low pH values (Wachter *et al* 2000). Figure 11(A) shows the normalized fluorescence emission of YFP as a function of pH and chloride concentration (Wachter *et al* 2000). Here we can see that the YFP is a suitable halide sensor at low pH and in fact has responses similar in magnitude to that seen for the dynamic quenching of fluorophores by chloride. One perhaps better probe for low chloride concentrations at the near neutral pH is another YFP, namely YFP-H148Q, figure 11(B) (Wachter *et al* 2000). Using this protein as a genetically encoded fluorescent probe, transport of halides across the cystic fibrosis transmembrane conductance regulator channel has recently been assayed, where a high level of sensitivity is reported in mammalian cells (Jayaraman *et al* 2000). As a result of their halide specificity, sensitivity, rapid response and the fact that YFPs can be used as genetically encodable halide sensors that may be targeted to specific organelles in living cells, it is likely that we are seeing the beginning of a whole new generation of bespoke 'intrinsic genetic halide sensors'.

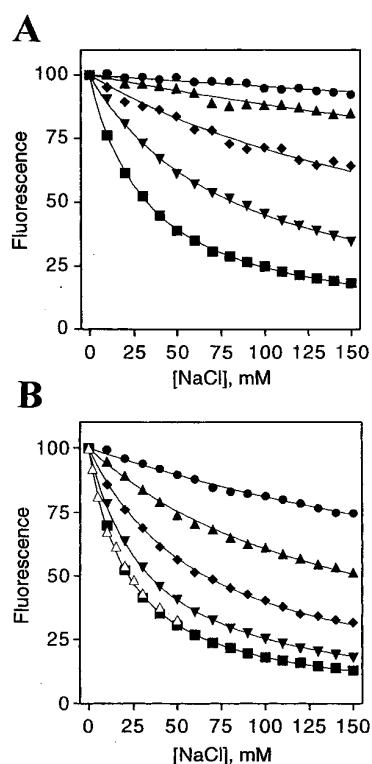


Figure 11. Normalized fluorescence emission of (A) YFP and (B) YFP-H148Q, as a function of pH and [Cl⁻] at constant ionic strength of 150 mM. The pH values were pH 8.0 (●), pH 7.5 (▲), pH 7.0 (◆), pH 6.5 (▼) and pH 6.0 (■). (B) includes the fluorescence emission of YFP-H148Q as a function of [I⁻] at pH 7.5 (△). Reproduced with permission from Wachter *et al* 2000, copyright © 2000, Academic Press.

3.3. Immobilized dye sensors

The use of dynamic fluorescence quenching of immobilized fluorophores for halide sensing was first reported by Urbano *et al* in 1984, where the need for immobilized dye halide sensors probably arose in fear of the invasive nature of extrinsic probes to some living and industrial systems. Since that time there have been several notable sensors whose quenching kinetics can be described by the various different models discussed in section 2 (Urbano *et al* 1984, Wyatt *et al* 1987, Zhu *et al* 1990, Jiwan and Soumillion 1997, Chen *et al* 1997, Geddes and Douglas 2000, Geddes 2000a,b, 2001). Immobilization usually involves the 'trapping' or covalent 'linking' of the halide sensitive fluorophore(s) either to the surface or within supports, which can be organic or inorganic polymers. The sensor membranes or films can then be used directly in steady-state or time-resolved quenching experiments, or even mounted on the tip of optical fibres to produce optrodes. A few examples are reviewed.

Urbano and co-workers immobilized both acridinium and quinolinium fluorophores onto glass supports, where glass was chosen over polymeric supports because it is not readily attacked by bacteria (Urbano *et al* 1984). Their sensor devices were able to detect chloride, bromide and iodide in solution in the pH range 4.2 to 7.4 (figure 12). We can see that the acridinium sensor, figure 12(A), is highly sensitive towards iodide and bromide but less so for chloride, and the

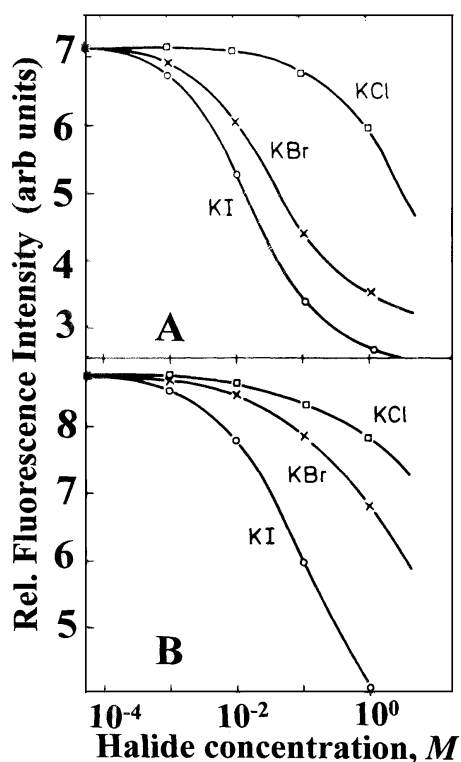


Figure 12. Relative fluorescence intensities (arbitrary units) of (A) acridinium and (B) quinolinium sensors as a function of halide concentration at 23 °C. Revised and reprinted with permission from Urbano *et al* 1984, copyright © 1984, American Chemical Society.

quinolinium sensor, figure 12(B), is of comparable sensitivity towards chloride, but only slightly more sensitive towards the other two halides. The errors in determination of halide in the concentration range 0.01–0.1 M were 1% for iodide and 1.5% for bromide. The error for the determination of chloride at concentrations around 100 mM, which is the normal level in blood, is reported as being $\approx 5\%$. Figure 13 shows the fluorescence response of the acridinium based sensor to (A) pure water, (B) 0.1 M potassium iodide, (C) 0.1 M potassium bromide and (D) 0.1 M potassium chloride. The 95% response time (the average time for the fluorescence signal to change by 95%) was ≈ 40 seconds. One can also see from figure 13 the reversibility of the sensor, where the fluorescence ‘returns’ as water is pumped over the surface of the sensor. Interestingly, total fluorescence quenching of the optical sensor does not occur, even when very high concentrations of quencher are used. They also observed that there was a 10–20% decrease in K_{SV} values for the immobilized fluorophores as compared to those determined for solution.

Optical halide sensors nearly always exhibit a significant reduction in the magnitude of the supported dye K_{SV} values as compared to those for solution. This reduction mostly reflects the limited mobility of the fluorophore and halide (lifetime changes are usually quite small) and the resulting lower probability of a quenching process, which reduces the dynamic range for quenching, and ultimately, the sensitivity towards halide. Ideally, supports for halide sensors should therefore

- allow the rapid and unhindered diffusion of halide

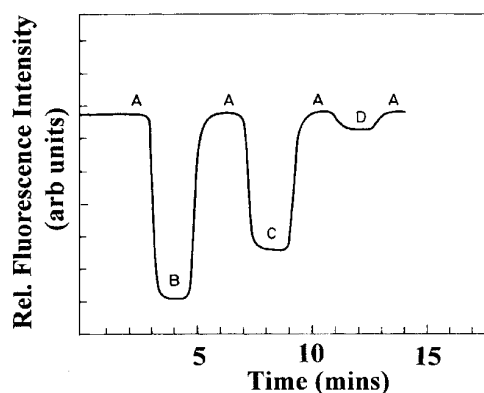


Figure 13. Fluorescence response of an acridinium sensor to (A) pure water, (B) 0.1 M potassium iodide, (C) 0.1 M potassium bromide and (D) 0.1 M potassium chloride. It is interesting to see that the response curves are not symmetric! Revised and reprinted with permission from Urbano *et al* 1984, copyright © 1984, American Chemical Society.

- provide for fluorophore immobilization, *in, on or between* the support(s)
- be chemically inert, i.e. no fluorophore–support–halide interactions
- be optically transparent in the region of interest
- have long ‘working’ (time in use) and ‘shelf’ (time stored without use) lives
- have good mechanical properties (for polymers, casting etc) and
- prevent the leaching of unbound⁴ fluorophore(s).

One recent study compares the K_{SV} values of a range of fluorescent probes, in free solution and unbound and bound in copolymer sensor films (Geddes and Douglas 2000). It is interesting to see from table 2, dyes E and F, that by increasing the crosslinking density of the copolymer support by covalently binding dyes to the copolymer, the magnitude of the K_{SV} values are significantly smaller, which the authors attribute to the restricted motion of the diffusing halide ions and the corresponding reduction in k_q (cf equations (2) and (4)–(6)). A similar effect is also observed with the harmaline type dyes, table 5, dyes C–F, and rhodamine B, table 6. By comparing these data with those reported by Urbano *et al* (1984), we can see that covalently binding dyes to the surface of a support has a less pronounced effect on K_{SV} values, 10–20% in their case, as compared to an $\approx 89\%$ reduction for dye E, table 2, when quenched by I^- . The bimolecular quenching constant, k_q , which as we have seen can provide information on dye accessibility and therefore polymer (support) structural information, has recently also been used to investigate the hydrophilicity and hydrophobicity of halide sensor supports (Geddes and Douglas 2000).

Jiwan and Soumilion constructed a halide sensor by immobilizing a hydrophobic dye (table 2, dye C) in a sol–gel matrix, where its hydrophobicity and hence compatibility within silica, reduced its leaching from the support when used in aqueous media (Jiwan and Soumilion 1997). The sol–gel

⁴ Unbound fluorophore refers to fluorophores dissolved within copolymer sensor films as compared to bound fluorophores, where fluorophores are covalently linked/attached within the supporting plastic sensor matrix.

matrix has several advantages over organic polymeric supports, such as a high photochemical and thermal stability, negligible swelling in liquids and very good optical transparency in the visible and near-ultraviolet domains. For their sensor, the quenching kinetics no longer followed the linear Stern–Volmer relationship which is described by equation (1), but instead could be adequately described by two populations of fluorophores, one a molecular and evenly distributed form and the other an aggregate form, where both had different decay times and different K_{SV} values towards aqueous halide, i.e. equation (30). Figure 14(A) shows the quenching of the heterogeneously doped sol–gel films by halide ions, where the solid lines represent fits to $I/I_0 = f_1/(1 + K_{SV1}[Q]) + f_2/(1 + K_{SV2}[Q])$, where f_1 and f_2 are the relative weighting factors. The K_{SV} values obtained from the fitting procedure can be seen in table 2, dye C, with fractional intensities, f_1 and f_2 of $f_1 = 0.75$, $f_2 = 0.25$; $f_1 = 0.83$, $f_2 = 0.17$ and $f_1 = 0.69$, $f_2 = 0.31$, for chloride, bromide and iodide respectively. The recovered K_{SV} values are in the order $I^- > Br^- > Cl^-$, which gives us some confidence in their interpretation. The sensor is capable of measuring chloride concentrations as low as 100 mM, in the pH range 6–9, with a very fast response time of less than 1 second (figure 14(B)).

Similarly, Wyatt *et al* have immobilized rhodamine 6G in three different supports in an attempt to elucidate critical factors in halide sensor design (Wyatt *et al* 1987). Figure 15 shows the Stern–Volmer plots for rhodamine 6G supported in three different supports. From these plots it can be seen that the Teflon optrode (C) (here an optrode is a fluorophore/support combination mounted on the tip of a fibre optic bundle) is much more sensitive than either resin based sensors and thus provides greater resolution in determining similar iodide concentrations. The K_{SV} values obtained from figure 15, assuming the data are described by equation (1), are shown in table 7. It is interesting that even though rhodamine 6G immobilized on Teflon has a much shorter lifetime than in the other optrodes, it provides a much stronger response to iodide: Teflon, $\tau_0 = 2.04$ ns; XAD-4 (resin bead), $\tau_0 = 5.14$ ns; XAD-4 (crushed resin), $\tau_0 = 5.16$ ns. Whilst this is explained by Wyatt and co-workers in terms of the better accessibility to the fluorophore molecules by iodide when they are immobilized in Teflon, it is generally observed that longer fluorescence lifetimes of fluorophores exhibit greater sensitivity towards halide, because a longer fluorescence lifetime increases the probability of an excited state deactivation quenching process. It is evident from figure 15 that equation (1) does not describe the quenching kinetics well and hence an alternative model describing two fluorophore populations, one inaccessible to halide, has been considered (figure 16) (see section 2.3). Assuming a linear relationship, the reciprocal of the y intercept of these plots gives the percentage of fluorophore which is *accessible* for quenching (equation (28)). These values are 93% for Teflon, 89% for crushed resin and 83% for resin beads, which complements data shown in figure 15 in that they also suggest the greater accessibility of the rhodamine 6G molecules to iodide by the greater magnitude of the K_{SV} values. Close examination of the data in figure 16 shows that the data are not exactly described by the linear relationship of equation (28) either, where the true behaviour is probably much more complicated than even this modified Stern–Volmer

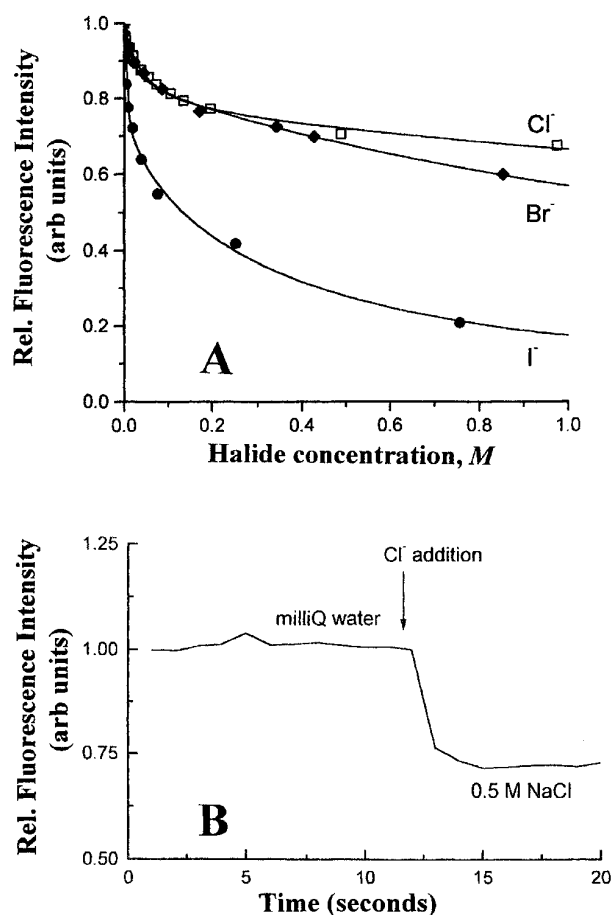


Figure 14. (A) The fluorescence quenching of a doped sol–gel film by aqueous halide ions. The solid lines represent fits to $I/I_0 = f_1/(1 + K_{SV1}[Q]) + f_2/(1 + K_{SV2}[Q])$, where f_1 and f_2 are the relative weighting factors (see table 2, dye C). (B) The very fast response of the sol–gel film to aqueous chloride. Revised and reprinted from Jiwan and Soumilion 1997, copyright © 1997, with permission from Elsevier Science.

equation assumes. Wyatt *et al* suggest that there may be a population of fluorophore molecules at an ‘intermediate stage of sequestration’ and, to circumvent this problem, one can add an exponent term to the Stern–Volmer equation, equation (36) (also described by Peterson *et al* 1984).

$$\left(\frac{I_0}{I} - 1\right)^m = K_{SV}[I^-]. \quad (36)$$

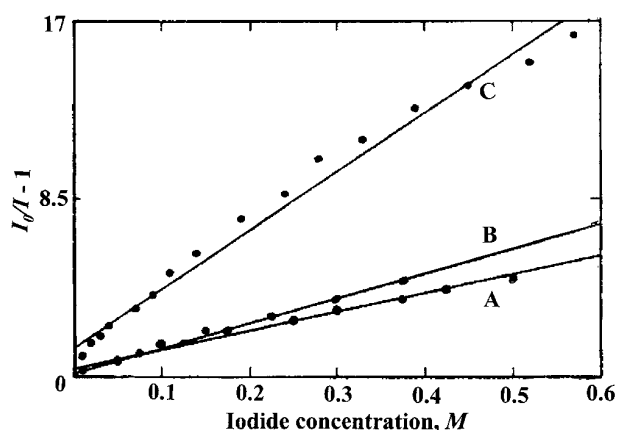
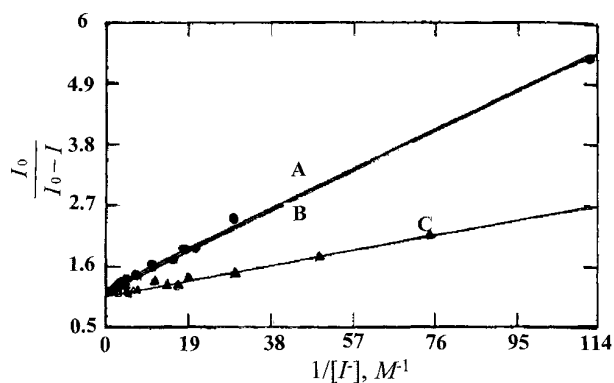
The parameters for the fit to equation (36), for the data shown in figure 15, can be seen in table 7. It is interesting to compare the K_{SV} values within table 7, where the values can be seen to significantly change depending on the Stern–Volmer model employed. For the Teflon optrode, Wyatt *et al* report a detection limit of 0.18 mM iodide, which is comparable to the value of 0.15 mM reported by Urbano *et al* for their sensors. The response times of these optrodes also parallels the ease with which I^- ions can diffuse, where the Teflon optrode gave the fastest 95% response time of ≈ 25 s as compared to ≈ 40 s reported by Urbano *et al*. Also, both sensors/optrodes are reported as showing noticeable interferences from nitrate, cyanide, bromate and isothiocyanate ions.

Table 7. K_{SV} values for three optrodes quenched by aqueous iodide, obtained by fitting the data in figure 15 to equation (1), and also the fitting of the data shown in figure 15, to equation (36).

Optrode ^a	$I^- K_{SV}$ (1)	$\left(\frac{I_0}{I} - 1\right)^m = K_{SV}[I^-]$ (36)		
		m	K_{SV}	r^2
A—XAD-4 resin bead	8.82 ± 0.96^b	1.51	20.0	0.998
B—XAD-4 crushed resin bead	11.61 ± 1.43^b	1.15	14.5	0.998
C—Teflon	28.7 ± 0.87^b	1.34	76.5	0.997

^a Here an optrode is a sensor device, where the fluorophore is immobilized on a support, which is incorporated on the tip of a fibre optic bundle. Data from Wyatt *et al* (1987).

^b Linear regression fits to the data in figure 15, between 0 and 0.6 M I^- (95% confidence intervals used).

**Figure 15.** Stern–Volmer plots for (A) XAD-4 resin-bead optrode, (B) XAD-4 crushed-resin optrode, and (C) Teflon optrode, quenched by iodide. Revised and reprinted with permission from Wyatt *et al* 1987, copyright © 1987, American Chemical Society.**Figure 16.** Modified Stern–Volmer plot (equation (28)) for (A) XAD-4 resin-bead optrode, (B) crushed resin optrode and (C) Teflon optrode quenched by aqueous iodide. Revised and reprinted with permission from Wyatt *et al* 1987, copyright © 1987, American Chemical Society.

The majority of optical halide sensors reported in the research literature incorporate one fluorophore in a support, which enables single halide concentrations to be determined. Some authors have used two or more individual sensors, each containing one dye, to simultaneously sense several halides, using the extended Stern–Volmer equation described in section 2.1.2. However in terms of simplicity, practicality and cost, it would be advantageous to have *one* sensor support

containing *multiple* dyes, to simultaneously sense halide. Such an arduous task to sense n halide concentrations would require

- n fluorophores sensitive to n halides in the same support
- *all* K_{SV} values would need to be different (see Wolfbeis and Urbano 1983) and
- the spectral emission peaks of the n fluorophores would need to be distinctly separate.

Whilst several authors have attempted this situation for $n = 2$, i.e. iodide and bromide sensing, one can clearly see the difficulties in trying to simultaneously sense Cl^- , Br^- and I^- with only one sensor.

Table 8 summarizes the detection limits, corresponding errors and response times of a few immobilized dye, fluorescence quenching based halide sensors. From table 8 we can see a typical lower detection limit for chloride of ≈ 10 mM, which is approximately five to ten times greater than that typically found in normal blood (Urbano *et al* 1984).

Another class of immobilized dye halide sensors are those based on FRET, which was described earlier in section 2.5. Recently Yang *et al* have described an optical iodide sensor based on FRET between anthracene, the donor molecule and 5,10,15,20-tetraphenylporphyrin (TPP), the acceptor (Yang *et al* 2000). When the probes are incorporated in a plasticized poly(vinyl chloride) (PVC) membrane, anthracene can non-radiatively transfer its emission energy to the TPP acceptor species, which then in turn fluoresces, where the significant spectral overlap criteria required for FRET exists between the donor emission and acceptor absorption spectra (figure 17(A)). Separately in both solution and membrane, anthracene is appreciably quenched by aqueous iodide ions whilst TPP is only slightly quenched. However, when a PVC sensor membrane containing both fluorophores is immersed in an aqueous iodide solution then stronger fluorescence quenching of TPP is observed. This is because the donor molecule is quenched, resulting in FRET being less efficient and therefore the fluorescence emission of TPP appears ‘significantly quenched’. Yang *et al* show that this donor–acceptor combination effectively increases the dynamic range of quenching, as compared to the individual quenching of the immobilized fluorophores (figure 17(B)). Yang *et al* suggest that this increased sensitivity is due to the additional quenching of the anthracene–TPP pair. Iodide concentrations can readily be determined by this sensor in the iodide concentration range $\approx 10^{-6}$ – 2.5×10^{-4} mol l^{-1} with a response time of less than 1 minute. The authors report a ‘working life’ of 100 quenching

Table 8. The lower detection limits, errors and response times (90 or 95%) of some optical halide sensors and optrodes, as reported in the research literature.

Sensor/optrode type	Halide	Detection limit	Response time	Reference
Acridinium and quinolinium dyes immobilized on the surface of glass supports	Cl ⁻	10.0 mM [3–5%] ^a	≈40 s ^b	Urbano <i>et al</i> 1984
	Br ⁻	0.40 mM [1.5%] ^a		
	I ⁻	0.15 mM [1%] ^a		
Quinolinium dyes immobilized in copolymer films	Br ⁻	1 mM [4%] ^c	30–60 s ^d	Geddes <i>et al</i> 1999b
	I ⁻	1 mM [2%] ^c		
Hydrophobic quinolinium dye in a sol–gel matrix	Cl ⁻	7.5 mM	≤1 s	Jiwan and Soumilion 1997
	Br ⁻	7.5 mM	≤3 s ^e	
	I ⁻	0.5 mM		
Quinine and harmane optrodes	Br ⁻	0.4 mM [<5%] ^c	≤120 s	Zhu <i>et al</i> 1990
	I ⁻	0.03 mM [<5%] ^c	≤230 s ^e	
Rhodamine 6G/Teflon optrode	I ⁻	0.18 mM	≈25 s ^f	Wyatt <i>et al</i> 1987

^a Percentage error in halide determination in the concentration range 0.01 to 0.1 M.

^b Average sensor response times (95%, seconds) for 0.1 M potassium halides.

^c Percentage error in halide determination at the detection limit.

^d Typical response time of sensors (90%, seconds) to molar iodide. These sensors are reported as having ‘shelf’ lives in excess of 2 years.

^e Reversible response time (i.e. the response to a decrease in halide concentration).

^f Response time (seconds) of the Teflon optrode to 14.0 mM iodide.

measurements with only an 8% drop in optrode fluorescence intensity (Yang *et al* 2000).

One other notable FRET based halide sensor was reported by Huber *et al* in 1998. Here, a plasticized PVC membrane contains a luminescent ruthenium complex placed in close proximity to the pH sensitive absorber bromothymol blue, BTB, along with an anion-selective carrier (Huber *et al* 1998). The response of the sensor is based on the *co-extraction* of both chloride and protons from an aqueous sample into the sensor membrane, which results in a large change in the absorption spectrum of the acceptor BTB. The absorption band of BTB overlaps significantly with deprotonated BTB and hence FRET occurs. If, however, chloride is co-extracted into the sensor membrane along with a proton, the dye is converted into the yellow phenolic form and hence FRET does not occur, resulting in a relatively longer lifetime of the complex, ≈1 μs, as compared to the quenched lifetime, ≈0.60 μs (figure 18). Huber *et al* state that the dynamic range of their lifetime based sensor can be adjusted via the sample pH and is from 30 to 180 mM Cl⁻ at pH 7.0, which is ideal for physiological samples. Their sensor array is also attractive in that

- it utilizes lifetime based measurements and is therefore unaffected by sensor membrane fluorescence intensity drifts/changes, due to either changes in the excitation intensity, dye degradation or dye leaching,
- it does not depend on the sensitivity of the detector and
- it does not require an expensive ultra-fast detection system, such as those required for *nano*- and *pico*-second lifetime measurements.

However, one disadvantage of their sensor is that it can only be used on real samples after pre-treatment with an appropriate buffer (Huber *et al* 1998).

3.3.1. Fluorophore leaching/sensor bleeding. A typical problem associated with immobilized fluorophore halide sensors is that of fluorophore leaching (sometimes also referred to as sensor bleeding). When a sensor is immersed in a halide

solution, the fluorescence intensity can sometimes fluctuate as the fluorophore slowly leaches from the sensor. Fluorophore leaching usually increases with temperature and in flow cells (Geddes *et al* 1999c) or ‘on-line’ type measurements where fluid is continuously washing over the surface of the sensor. In a recent study, Geddes and Douglas (2000) have studied the extent of both bound and unbound fluorophore leaching in different copolymer sensor films where the temperature, and both the percentage and type of polymer crosslinking agent used, were varied. Figure 19 shows the static leaching of unbound and bound rhodamine B from two identical copolymer films at 20 °C, pH 10. The percentage dye remaining in films, of the same thickness, was calculated from the decrease in the absorbance of the films as a function of time. Figure 19 shows that by covalently binding rhodamine B to the copolymer sensor film (through an ester linkage), dye leaching is eliminated, but from table 6 we can see that the magnitude of the I⁻ K_{SV} value and hence the dynamic quenching range is also significantly reduced. Clearly for optical halide sensors based on immobilized fluorophores a compromise between dye leaching and dynamic range needs to be achieved. It is interesting to note that by lowering the solution pH from 10 to ≈1 resulted in dye leaching, which is thought to be a result of the hydrolysis of the ester linkage and the subsequent *unbinding* of the dye. Hence meticulous studies of dye attachment need to be undertaken, especially if sensors are to be used in living systems.

If sensor ‘bleeding’ is inevitable, then lifetime measurements, which do not depend on total fluorescence intensity, or the use of a reference sensor film, should be considered. Geddes has suggested that for bleeding sensors one can also compensate for dye loss by continuously measuring the fluorescence intensity of the blank solution, i.e. I₀ (equation (1)). This is possible because the calculated halide concentration is dependent on the ratio I₀/I, rather than on the absolute fluorescence intensity of the sensor film (Geddes 2000b).

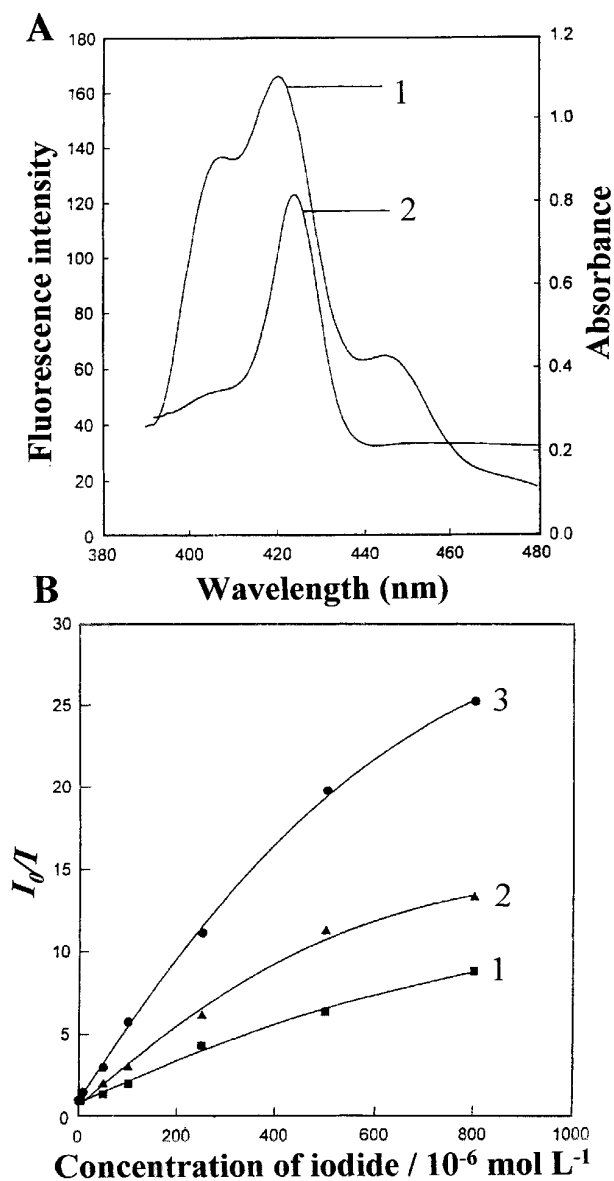


Figure 17. (A) Emission (1) and absorption (2) spectra of anthracene and TPP respectively in a PVC membrane. (B) Sensor membrane Stern–Volmer plots for the quenching of iodide by (1) TPP excited at 423 nm, fluorescence emission monitored at 657 nm, (2) anthracene excited at 373 nm, fluorescence emission monitored at 420 nm and (3) the anthracene–TPP system excited at 373 nm and the fluorescence emission monitored at 657 nm. Yang *et al* 2000. Revised and reproduced by permission of the Royal Society of Chemistry.

3.3.2. Halide sensor calibration, stability and interference.

Most halide sensor devices require calibration before use as it is frequently observed that optrodes with supposedly the same composition rarely give an identical response (Zhu *et al* 1990). Zhu and co-workers have immobilized the quinine and harmane fluorophores in cellulose and subsequently produced two fibre optic halide sensors for the simultaneous determination of aqueous bromide and iodide ions. Their sensor array utilizes the extended Stern–Volmer equation described earlier in section 2.1.2. Whilst studying the possible interference by ions such as nitrate (NO_3^-), copper (Cu^{2+}) and magnesium (Mg^{2+}) on the response of three quinine optrodes in

the presence of 10 mM bromide, the authors observed the three Stern–Volmer plots to have different intercepts on the $I_0/I - 1$ axis, i.e. at zero quencher concentration (figure 20). Zhu *et al* attribute these different intercept values to the homogeneity of distribution of the cellulose powder in the optrode and possibly, further, upon the inhomogeneity of dye molecules in the cellulose powder. As each optrode responds differently at zero analyte concentration, then for practical applications the optrodes would need to be calibrated *individually* before use. Recently, Geddes has also investigated this effect and has reported the homogeneous distribution of SPI (table 5, dye B) within a polymeric support. His conclusions are based on the fact that identical zero halide concentration I_0/I values are obtained for the sensors. It is therefore envisaged that mass halide sensors can be produced, requiring only one initial calibration, thus minimizing production costs (Geddes 2000b). Given that there are only a few reports of this effect in the research literature (with respect to halide sensing), it is difficult to draw any conclusions, but it is likely that dye inhomogeneity and therefore the need for individual halide sensor calibrations will depend on specific dye and sensor support interactions.

The stability of fluorophores in a support (as well as the support itself), during irradiation, is also an important factor in halide sensor design. This is particularly important in continuous ‘on-line’ type measurements where the fluorescence intensity can change as fluorophores degrade over a period of time. In single or quick measurements this is not as crucial, as long as any degradation products do not interfere with the quenching kinetics, and for steady-state fluorescence measurements sufficient fluorophore is present so that the signal to noise ratio does not become problematic. For signal corrections, then similarly to compensate for dye leaching, a reference sensor or lifetime measurements should be employed.

For the sensors described by Urbano *et al* (1984), irradiation with a 250 W xenon arc lamp with a 20 nm band-pass resulted in an approximately 15% decrease per hour in the fluorescence signal, although, as the authors suggest, the excitation intensity used in their work was approximately ten times greater than that required for practical sensor applications. Similarly, Geddes has used a 100 W stabilized tungsten halogen lamp with a 320–510 nm band-pass filter, and, also using SPQ, reports no change in fluorescence signal with time (Geddes 2001). This improvement in sensor stability has been attributed to the lower power of the excitation source.

Interferences, aqueous ions which can bias the fluorescence quenching kinetics of a system, need to be studied before a sensor is applied in practice, so that the contribution (or not) to the overall quenching process can be accounted for in the halide analysis. Fortunately, the model described by equations (7)–(16), which allows the determination of two or more quenchers in one solution, also has the added attraction of mathematically describing interferences (by simply introducing (an)other term(s) into the Stern–Volmer equation), providing the interference K_{SV} value is predetermined from plots of I_0/I against [interference], and that both halide and the interference quench independently.

3.3.3. Halide sensor response times. By observing the rate of change of fluorescence intensity of an immobilized

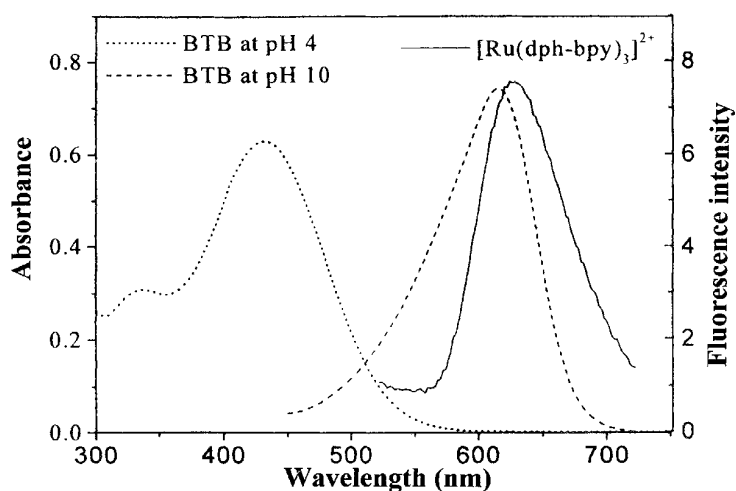


Figure 18. pH dependent absorption spectra of BTB in pH 4 and pH 10 aqueous buffers, and the fluorescence emission spectrum of the ruthenium complex. The absorption band at 616 nm increases with pH. Hence energy transfer occurs if BTB is deprotonated due to the increased spectral overlap with the emission band of the ruthenium complex. Reprinted from Huber *et al* 1998, copyright © 1998, with permission from Elsevier Science.

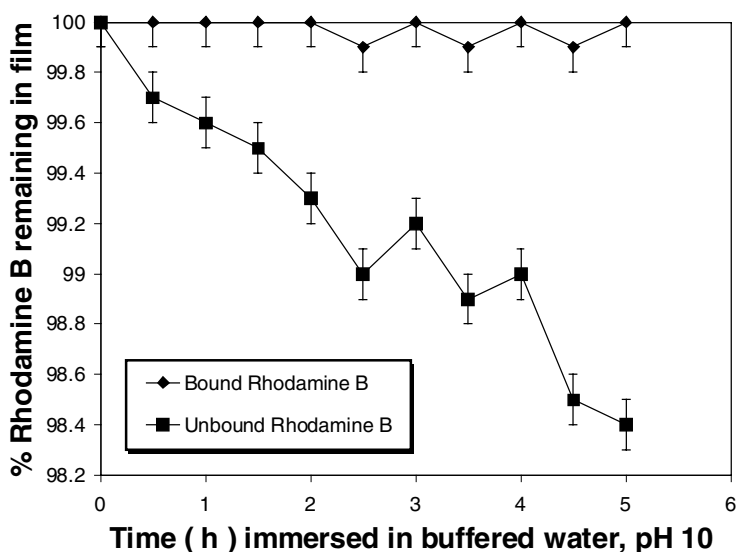


Figure 19. Static leaching of rhodamine B unbound and bound sensor films in buffered water, pH 10. A solution pH of 10 was employed as the sensors were used for halide sensing in mildly alkaline photographic processing solutions. The films had the same initial thickness, ≈ 50 micrometres, and same initial absorbance. Reproduced with permission from Geddes and Douglas 2000, Copyright © 2000, John Wiley & Sons, Inc.

dye halide sensor in the presence of aqueous halide, one can determine the response time of the sensor. Response times are typically quoted as the time for either a 90 or 95% change in sensor fluorescence intensity, as compared to the fluorescence intensity in the absence of quencher (Urbano *et al* 1984). From table 8 we can see that typical response times of halide sensors to modest halide concentrations are < 1 min, which is ideal for both physiological and industrial ‘on-line’ measurements. Similarly to k_q values, sensor response times can also give an indication about the accessibility of halide to the fluorophore and can therefore report sensor support structural information. In one recent study, Geddes observed that the response times of a plastic halide sensor to both bromide and iodide were identical, which at first may seem quite surprising, as one would expect a quicker response to bromide than iodide, because of its relatively smaller ionic

volume and low mass. Geddes attributed this effect to the microscopic structure of the halide sensor, where a significant degree of polymer crosslinking must be present to reduce both response times to a similar extent. Interestingly, iodide showed a longer reversible response time as compared to bromide, when the sensor was washed with a non-quenching solution, which is consistent with the more difficult removal of the heavier iodide ion (Geddes 2000b). Due to the more difficult removal of halide, reversible response times, the time for 90 or 95% fluorescence recovery, are often substantially longer than the response time. Factors, which typically effect sensor response times include

- the temperature of the halide solution
- the flow rate or pressure of the quenching solution (see Okamoto and Teranishi 1984, Okamoto 2000)

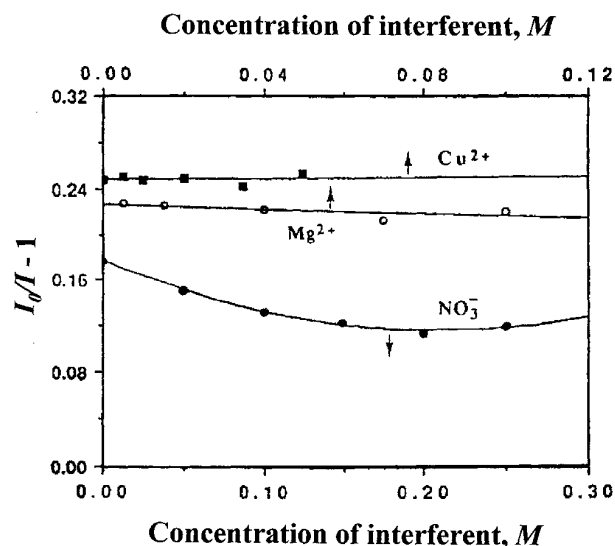


Figure 20. The interference of several ions on the response of a quinone optrode in the presence of 10 mM bromide. Revised and reproduced with permission from Zhu *et al* 1990, copyright © 1990, Society for Applied Spectroscopy.

- the sensor thickness and internal pore volume (i.e. for sol-gel supports)
- the swelling properties, i.e. hydrophilicity, and crosslinking density of the support (i.e. for plastic supports) and
- the time required to fill flow cells, sometimes referred to as the 'null' or sensor 'dead' time (see Geddes *et al* 1999c).

Whilst 90 or 95% fluorescence intensity changes typically occur <1 min, it is frequently observed that 100% fluorescence quenching of immobilized dye halide sensors never occurs, even after very long times using perverse halide concentrations. Many authors have attributed this to 'buried' fluorophore in the support, which is inaccessible to diffusing halide, thus creating 'background' sensor fluorescence. As a result, quenching kinetics often follow the model described in section 2.3 for one accessible and one inaccessible fluorophore.

3.3.4. Sensing the anaesthetic 'halothane' (organic/bound halides). The quenching of fluorophores by alkyl or aryl halides has been studied many times (Davis 1973, Behera and Mishra 1993, Behera *et al* 1995b, Zhang *et al* 1997, Lakowicz 1999). Heavy-atom fluorescence quenching is generally observed with the iodides and bromides, but less efficiently for the chlorides. Polychlorinated alkanes, with more than one chlorine moiety at the same carbon atom, are generally found to be weaker quenchers than the monochlorides, and the fluoroalkanes are considered almost inert (Wolfbeis *et al* 1985). One particular alkylhalide that is of particular interest to medicine is the inhalation narcotic, *halothane* (CF_3CHBrCl), which is frequently used in anaesthetics. There are quite a few commercially available monitors for halothane, such as 'EMMA', which is based on the absorption of halothane by a thin film of oil, where the mass of film, and hence percentage of halothane, is monitored using a piezoelectric crystal (Wolfbeis *et al* 1985). The Datex anaesthetic agent monitor measures halothane in air via its characteristic IR absorption. Other laboratory analytical procedures for measuring halothane in

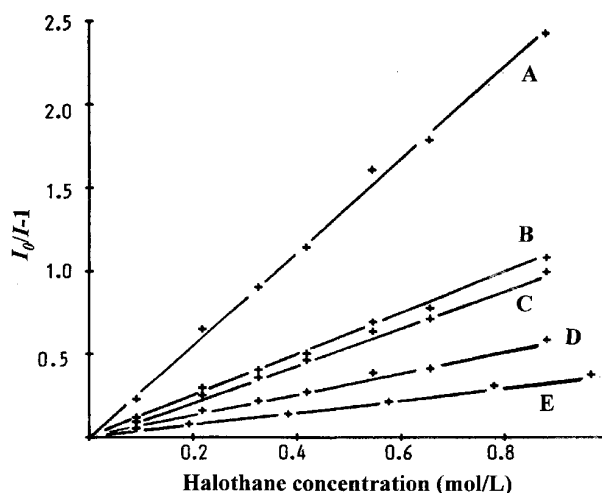


Figure 21. Stern-Volmer plots of the quenching of polycyclic aromatic hydrocarbons by halothane in methanol at 23 °C. The fluorophores and corresponding Stern-Volmer quenching constants are (A) anthracene, 2.75, (B) fluoranthene, 1.20, (C) dibenz[a,h]anthracene, 1.12, (D) decacycene, 0.62, and (E) perylene 0.39 M^{-1} . Reprinted with permission from Wolfbeis *et al* 1985, copyright © 1985, American Chemical Society.

breath gas and blood have also been described such as gas chromatography (Dueck *et al* 1978), electrochemical sensing (Hall *et al* 1988, Caruana 1998) and UV spectroscopy (Diprose *et al* 1980, Howie and Hawkins 1993), to name but a few. The quenching of fluorescence has also been used to monitor halothane since the bromine moiety of halothane can heavy-atom quench the fluorescence of certain fluorophores (Lamb 1978, Wolfbeis *et al* 1985, Sharma *et al* 1992, Howie and Hawkins 1993) (figure 21). Subsequently, the diffusion of halothane through membranes has been studied using the quenching of pyrene fluorescence (Washington *et al* 1984), as well in different polymeric sensor supports containing various fluorophores (Wolfbeis *et al* 1985, Howie and Hawkins 1993).

In anaesthetic practice, halothane is mostly delivered in combination with elevated levels of oxygen. Initially, during the 'flood' phase, 1–3% halothane is contained in the inhalation gases along with 30–50% oxygen, the remainder being N_2O . After this period, the halothane concentration is reduced to 0.6–1.0% (Wolfbeis *et al* 1985). Since both halothane and oxygen can act as collisional quenchers, then any oxygen or halothane fluorescence quenching based sensors monitoring this practise will inevitably display moderately complex kinetics. Wolfbeis *et al* have investigated this problem and have subsequently developed fluorescence quenching based sensors to determine halothane concentrations at a constant oxygen concentration, such as for the situation in air, and also in the presence of varying concentrations of oxygen, such as in blood or anaesthetic supply gas. Their *two sensor technique*, which utilizes the 'extended Stern-Volmer equation', allows the determination of halothane, or oxygen, or both with a precision of $\pm 5\%$ for halothane and $\pm 3.5\%$ for oxygen in the concentration ranges encountered in anaesthetic practise (Wolfbeis *et al* 1985).

For the situation in air, equation (7) can be used to describe the dynamic quenching of a fluorophore by both halothane [H] and oxygen [O], providing that both quenchers

act independently, i.e.

$$\frac{I_0}{I} - 1 = {}^H K_{SV}[\text{H}] + {}^O K_{SV}[\text{O}] \quad (37)$$

where ${}^H K_{SV}$ and ${}^O K_{SV}$ are the Stern–Volmer constants for halothane and oxygen respectively. When halothane is added to a gas such as air, the concentration of oxygen is subsequently reduced according to

$$[\text{O}] = x \left(1 - \frac{[\text{H}]}{100} \right) \quad (38)$$

with x being the initial concentration of oxygen (%) and $[\text{H}]$ the concentration (%) of halothane. Wolfbeis *et al* have shown that combination of equations (37) and (38) gives

$$\frac{I_0}{I} - 1 = [\text{H}] \left({}^H K_{SV} - \frac{x {}^O K_{SV}}{100} \right) + x {}^O K_{SV} \quad (39)$$

which describes a straight line of the type $y = a[\text{H}] + b$, with the gradient, a , equal to $({}^H K_{SV} - x {}^O K_{SV}/100)$ and intercept b equal to $x {}^O K_{SV}$. Hence a plot of $[\text{H}]$ against $(I_0/I - 1)$ enables a and b to be determined, providing that the oxygen concentration of the supplying gas remains constant. If the supplying gas is air, then $x \approx 21$. Figure 22 shows Stern–Volmer plots obtained by plotting $(I_0/I - 1)$ against $[\text{halothane}]$ for decacyclene in a silicone support under (A) oxygen, (B) air and (C) nitrogen. The linearity of the plots demonstrates the independent action of the two quenchers and allows the simple simultaneous determination of the two quenching constants (Wolfbeis *et al* 1985). Figure 23 shows the fluorescence response of solubilized decacyclene in silicone towards halothane and oxygen, where the authors state that the silicone rubber is an ideal support because of its good solubility and high permeability for halothane and oxygen. From the response curve of the halothane/oxygen sensor (figure 23), we can see that at 0% halothane the fluorescence signal is greatest, but drops $\approx 21.3\%$ when 5.5% halothane is admitted to the gas flow. At lower halothane concentrations the signal increases and eventually reaches the initial value again when no more halothane is present (Wolfbeis *et al* 1985). With air as the supply gas then the fluorescence signal decreases $\approx 20.6\%$ with respect to the signal under nitrogen because of the quenching by oxygen. On addition of 5.5% halothane the fluorescence signal diminishes further owing to the additional quenching by halothane. The authors report that the halothane/oxygen sensor is fully reversible with a 90% response time of 15–20 s.

For the situation of different amounts of oxygen in the supply gas equation (37) is no longer valid and further use must be made of the extended Stern–Volmer equation described in section 2.1.2. For this problem, Wolfbeis *et al* used two sensors each with different sensitivity and different quenching constants for halothane and oxygen. For sensor A, the fluorescence signal is given by $\alpha = (I_0/I - 1)$, and sensor B displays a different signal, $\beta = (I_0/I - 1)$. By coating one of the sensors with polytetrafluoroethylene (PTFE), which makes sensor B specific for oxygen only, then, similarly to equations (14) and (15), the extended Stern–Volmer equations for both halothane and oxygen respectively are

$$[\text{H}] = \frac{(\alpha {}^O K_b - \beta {}^O K_a)}{{}^H K_a {}^O K_b} \quad (40)$$

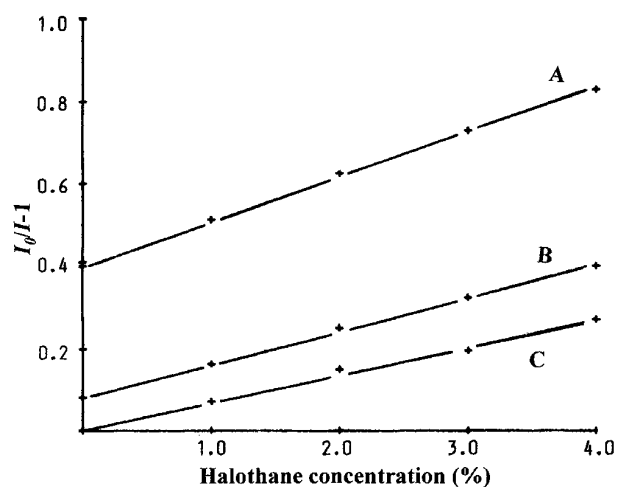


Figure 22. Stern–Volmer plots obtained by plotting $(I_0/I - 1)$ against halothane concentration under (A) oxygen, (B) air and (C) nitrogen. Wolfbeis *et al* clearly demonstrate the independent action of the two quenchers by the linearity of the plots. Reprinted with permission from Wolfbeis *et al* 1985, copyright © 1985, American Chemical Society.

$$[\text{O}] = \frac{\beta}{{}^O K_b} \quad (41)$$

where ${}^H K_a$ is the halothane quenching constant for sensor A and ${}^O K_a$ and ${}^O K_b$ are the corresponding oxygen quenching constants for sensors A and B respectively. Hence, providing that the quenching constants are predetermined, only α and β have to be measured to determine the halothane and oxygen concentrations.

One further refinement to their sensing mechanism was to use two *identical* sensors, one of which was PTFE covered. In this case the two quenching constants for oxygen become *identical*, which leads to a final equation that describes the relation between the two sensor signals and the halothane concentration

$$[\text{H}] = \frac{(\alpha - \beta)}{{}^H K_a} \quad (42)$$

Wolfbeis *et al* suggest that this sensor array has potential applications in

- the continuous *in vivo* monitoring of halothane in blood with fibre optic catheters during operations,
- the continuous monitoring as well as the *in vivo* measurement of oxygen in the presence of halothane and
- the continuous monitoring of breath gases (Wolfbeis *et al* 1985).

3.4. Experimental precautions and considerations in halide sensing

Whilst quenching experiments are generally straightforward, there are a few potential problems that researchers should be aware of.

- One should always use the highest purity quencher possible, especially when working at high quencher concentrations, as they may contain fluorescent impurities.

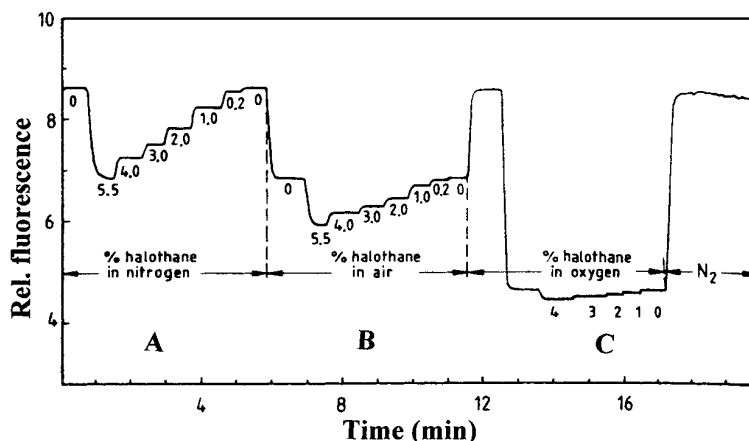


Figure 23. The fluorescence response (arbitrary units) of the halothane/oxygen sensor (0.05% decacyclene in silicone rubber) to different concentrations of oxygen and halothane. Range **A**, halothane in pure nitrogen, range **B**, halothane in air, and range **C**, halothane in oxygen. Reprinted with permission from Wolfbeis *et al* 1985, copyright © 1985, American Chemical Society.

- One should always check the emission spectrum at low signal-to-noise ratios, i.e. at maximum quenching, as any contribution from a background fluorescence source may become significant.
- One should always be aware that the position of the Rayleigh and Raman scatter bands are independent of the quencher concentration but the contribution from scattered light will always increase with the extent of quenching.
- A constant ionic strength needs to be maintained during quenching experiments as described in section 2.6.
- When using aqueous iodide, one should be aware that I_2 can be photochemically formed and hence the use of a reducing agent should be considered, i.e. $2I^- + \frac{1}{2}O_2 + H_2O + h\nu \rightarrow I_2 + 2OH^-$ (Sivaraman and Rajeswari 1983).

3.4.1. Halide concentration range studied. We have seen that a typical upper limit used in halide quenching studies is ≈ 0.1 M. The concentration range (>0 – 0.1 M) is typically used because the signal-to-noise ratio of the system is not a problem for the quenched sample, the system requires minimal experimental corrections, halide concentrations in human physiology and many industrial processes are typically <0.1 M and most systems will show a linear dependence of I_0/I on $[Q]$, at halide concentrations <0.1 M. We can see this quite clearly if we consider the nonlinear examples displayed in figures 6–8, where most could be considered linear over this concentration range, particularly when we realize that no experimental noise is present in the simulated data. The consequence of such a linear analysis over this small concentration range is the incorrect estimation of the K_{SV} or K_S values as well as the incorrect description of the quenching kinetics and their physical meaning. We can see this in figure 24, which shows the halide quenching range 0.01–0.1 M of figure 7(A), when $K_{SV1} = 1 \text{ M}^{-1}$. Assuming that only a single species is collisionally quenched, i.e. the quenching kinetics are described by equation (1), then the sole K_{SV} value (calculated by linear regression) is $\approx 4 \text{ M}^{-1}$ (with $R^2 = 0.996$) instead of the four parameters used to generate this synthetic data, i.e. $K_{SV1} = 1 \text{ M}^{-1}$, $K_{SV2} = 10 \text{ M}^{-1}$ and $f_1 = f_2 = 0.5$. Therefore for a correct and meaningful interpretation of the quenching kinetics of a system, and also

for the accurate determination of K_{SV} values for immobilized dye sensors, quenching studies should be carried out to higher quencher concentrations with a greater data density. To further test the (non)linearity of quenching data, residuals from any fitting procedure should also be examined to ensure against systematic behaviour.

3.4.2. Steady-state or time-resolved measurements?

Fluorescence measurements are broadly classified into two main types of measurement, steady state and time resolved. Steady-state measurements are performed with constant illumination and the subsequent constant observation of the fluorescence signal, whereas for time-resolved measurements the sample is exposed to a very short pulse of light and the intensity decay recorded with a high speed detection system (Birch and Imhof 1991). The steady-state observation is simply an average of the time-resolved phenomena over the intensity decay of the sample (Lakowicz 1999). It is well known that the intensity decay contains useful information that can be lost during this time averaging process and hence time-resolved measurements are preferred. Due to the relative complexity and expense of early time-resolved instrumentation, many early halide sensing measurements were made using steady-state type devices. However, due to the dramatic cut in instrumentation costs over the last approximately five years, time-resolved equipment is now commonplace in many laboratories and as a result ever more fluorescence lifetime based sensors are emerging (Szmecinski and Lakowicz 1994, Lakowicz 1995, Thompson 1997, Lippitsch *et al* 1997). The author summarizes the relevant advantages of both techniques with respect to their roles in optical halide sensing.

In the last section the author demonstrated that if quenching data are not collected to a high enough concentration of quencher, then a linear regression could adequately fit the data, and an erroneous K_{SV} value obtained (figure 24). If the trend in the I_0/I data for a single emitting species is nonlinear, then when using steady-state measurements a problem will arise in trying to decide which static quenching process is causing the effect, as both the ground state complex and sphere of action quenching models can fit the data equivalently,

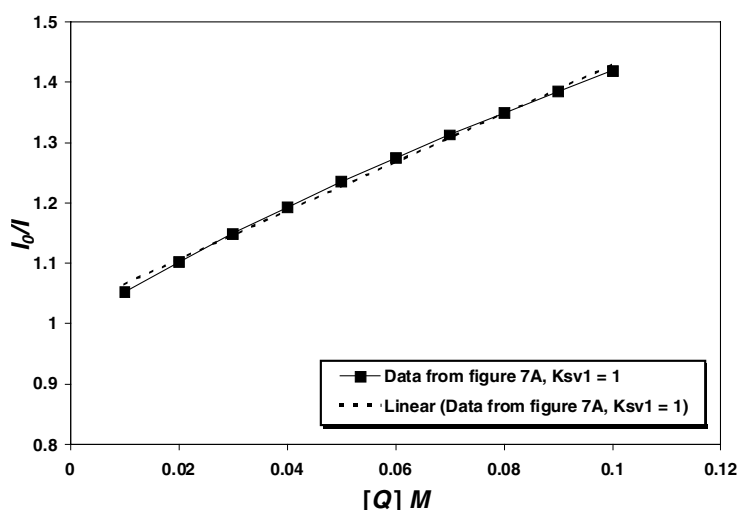


Figure 24. Simulated data from figure 7(A) when $K_{SV1} = 1 \text{ M}^{-1}$ in the halide concentration range 0.01–0.1 M. For a least squares linear regression analysis (the dotted line), the K_{SV} value obtained is $\approx 4 \text{ M}^{-1}$ with $R_2 = 0.996$.

especially at low $[Q]$. If multiple species are present then it is difficult to find unique solutions since too many parameters have to be evaluated and further information is therefore required. This additional information can easily be determined from complimentary time-resolved measurements, which can provide K_{SV} values for a single species and, depending on the number of emitting species, may be able to obtain $K_{SV}(i)$ and $f(i)$ values for heterogeneous systems.

For dynamic quenching of a single species, then the K_{SV} value obtained by I_0/I (equation (1)) must be the same as the K_{SV} value determined by τ_0/τ (figure 4). If, however, the K_{SV} term obtained from steady-state measurements is larger than the K_{SV} value obtained from time-resolved data, then an additional static mechanism is implicated. In contrast, if a single species has been verified by time-resolved experiments, but static quenching is also occurring, then the K_{SV} value obtained from the τ_0/τ plot will represent the dynamic component only. For multiple species, the only way to analyse steady-state data is to predetermine the $K_{SV}(i)$ and $f(i)$ values from time-resolved experiments, otherwise there are too many parameters to iterate and unique quenching solutions cannot be found. Hence one can see that to completely understand a quenching system it is important to obtain as much information as possible and therefore both steady-state and time-resolved quenching studies need to be performed.

As well as being useful to distinguish between different halide quenching mechanisms, time-resolved measurements (lifetime based sensing) also have one other important advantage over steady-state (quantitative intensity) measurements. Lifetime based sensing is independent of the intensity of the signal, providing that it is large enough to be measured. This allows for measurements to be unperturbed by dye degradation or even dye leaching from a sensor support, which, as the author has shown, are typical problems inherent with immobilized dye sensors. Another advantage of using lifetime based measurements is that they are typically independent of inner-filter effects, because lifetime measurements are independent of total light intensity. Below $\approx 300 \text{ nm}$ the halides have a measurable absorbance and so steady-state quenching measurements would have to be

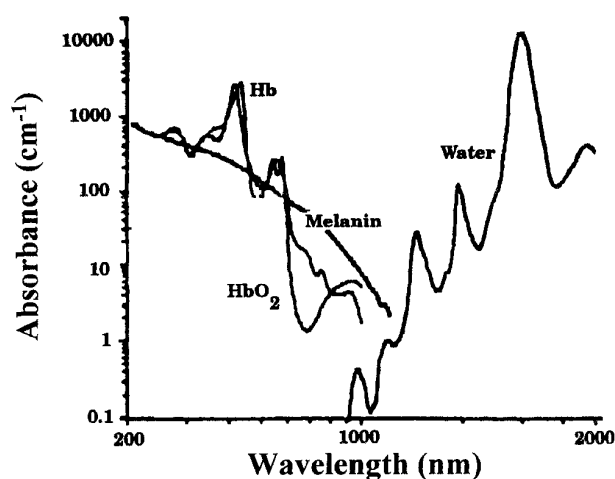


Figure 25. The near-infrared therapeutic window of 600–1000 nm. Hb, haemoglobin. Revised and reproduced with permission, from the *Annual Review of Physical Chemistry*, Volume 47 © 1996 by Annual Reviews.

corrected for the apparent decrease in fluorescence intensity due to the inner filter effect (Borissevitch 1999). Similarly, if the lifetime is measured by phase modulation (Lakowicz and Gryczynski 1991), the values are expected to be independent of intensity.

3.5. Opportunities for 'multiphoton' halide sensing

One typical problem of halide sensing using fluorescence quenching in biological applications has been finding/designing dyes which are both highly sensitive to halide ions at physiological concentrations and which also accommodate the optical properties of water and tissues. In general the auto-fluorescence from tissues or any biological sample is lower at longer excitation wavelengths. At longer wavelengths one also avoids the absorption of haemoglobin and melanin but unfortunately there are very few halide sensitive probes that both absorb and emit within this region (Andrews-Wilberforce and Patonay 1989). The region of low absorption from 600 to 1000 nm is sometimes called the therapeutic range

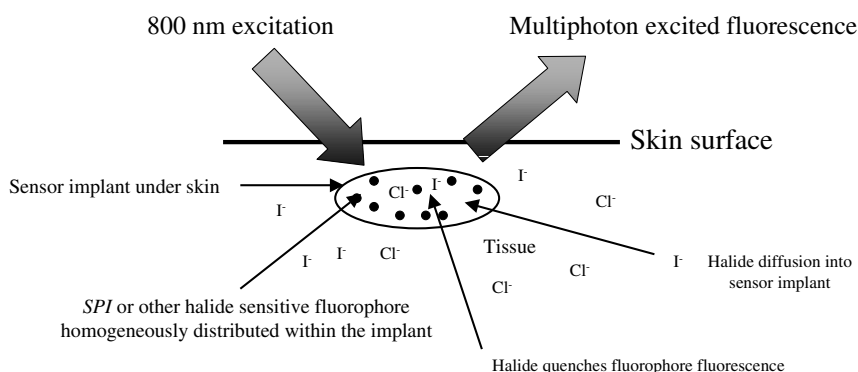


Figure 26. The principle of multiphoton transdermal halide sensing. Reprinted from Geddes 2000b, copyright © 2000, with permission from Elsevier Science.

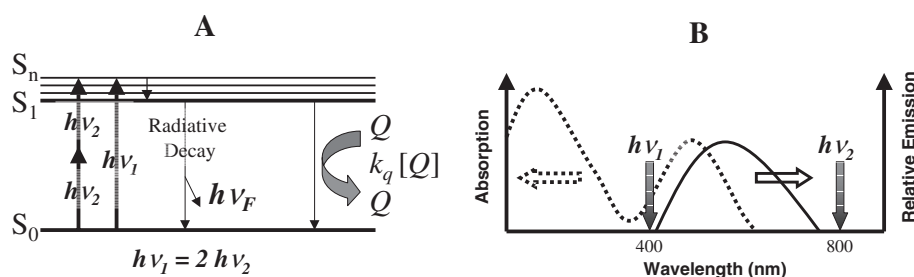


Figure 27. (A) Modified Jablonski diagram for two photon excitation, (B) illustration of two photon excitation for a fluorophore where the dotted line and bold lines represent the one-photon absorption and emission spectra of the fluorophore respectively. In energy terms, two photons $800 \text{ nm} = 1 \text{ photon } 400 \text{ nm}$.

(figure 25) (Richards-Kortum and Sevcik-Muraca 1996). It has been suggested by Geddes that it may be possible to overcome this problem using the multiphoton excitation of current probes, such as *SPI* (Geddes 2000b), using a near-infrared excitation source, such as a 800 nm femtosecond Ti:sapphire laser (Volkmer *et al* 1997). Near-infrared excitation also has the additional attractions of reduced dye and sample degradation and the reduced scattering of the excitation light, λ^{-4} dependence. Further, Geddes suggests that it may be possible to transdermally sense and hence continually monitor physiological halide in the future, using a sensor implant incorporated just under human skin (figure 26). This would be of significant importance to medicine as discussed in section 1.2. In practice it should be possible to adopt this principle to most other quenching systems, which have intrinsic or extrinsic fluorescent probes.

The principle of multiphoton excitation is shown in figure 27 (Lakowicz 1997). Here, a fluorophore absorbs two long wavelength photons at the same instant (within 10^{-15} – 10^{-16} s) to reach the shorter wavelength first excited singlet state (or higher state that then relaxes to S_1). Unlike one-photon absorption, where the amount of light absorbed is proportional to the intensity of the incident light and therefore the emission intensity is directly proportional to the excitation intensity (*the Beer-Lambert law*), for two photon excitation, the emission depends on the square of the incident light intensity. Similarly, for n photon excitation, the emission depends on the n th power of the incident intensity. Multiphoton excitation is by no means a new concept: in fact the possibility of two-photon absorption was predicted in the 1930s, but it was not until the invention of lasers that the phenomenon was observed. More recently, the use of multiphoton excitation has been particularly useful in

fluorescence microscopy (White *et al* 1991), since localized excitation occurs only at the focal point of the excitation beam (Lakowicz 1999).

4. Summary

Optical halide sensing using fluorescence quenching methods is a versatile analytical technique for the determination of halide ions or organic halides. Measurements can have several advantages over other techniques, e.g. ion-selective electrodes, in that halide concentrations can be determined in very small sample volumes, no pre-treatment of samples is generally required and measurements can be non-invasive, very quick or even continuous. However, similarly to some ion-selective electrodes, fluorescence quenching is not a particularly selective process and other halides, pseudohalides, heavy atoms or even dissolved molecular oxygen can perturb measurements (section 3.1.1). Fortunately interferences can be readily corrected for, provided that the fluorophores response to the interference is known (section 3.3.2).

Another advantage of halide sensing using fluorescence quenching is that halide concentrations can be determined using either intrinsic or extrinsic fluorescence probes. However, the addition of extrinsic probe molecules to living systems and *some* industrial processes is not desirable and therefore, for physiological samples, intrinsic fluorescent probes, such as protein tryptophans or even yellow or green fluorescent proteins, are sometimes preferred (section 3.2.1). An alternative to the introduction of extrinsic probes has been to immobilize halide sensitive fluorophores *onto* or within a support (section 3.3), which, when immersed into the desired sample, readily allows the diffusion and therefore the sensing

of aqueous halide ions, or, in the case of halothane, gaseous alkylhalide (section 3.3.4).

Immobilized dye halide sensors have been semi-successful in preventing the contamination of samples with extrinsic probes, although many sensors do experience a degree of dye leaching (section 3.3.1). However, whilst trying to trap fluorophores within a sensor matrix to reduce leaching one inevitably hinders the diffusion of halide and therefore the sensitivity and dynamic range of the sensor. Consequently, many halide sensors consist of covalently bound fluorophores *to* or *within* the support, which allows the density of the support to be reduced (for organic polymers—the crosslinking density), with the intention of increasing halide diffusion rates, k_q , and ultimately the K_{SV} value. Fortunately the halide sensitivity of many probes affords for the reduction when immobilized, where the many sensors reported can adequately sense physiological and industrial halide concentrations with rapid response times and reasonable ‘working’ and ‘shelf’ lives.

Although contamination of samples with extrinsic probes can be significantly reduced or eliminated by immobilization, one resultant disadvantage is that sensor quenching kinetics can be rather complex and, to fully understand halide quenching kinetics and therefore give physical meaning to quenching parameters, both time-resolved and steady-state analysis needs to be performed (section 3.4.2). Since fluorescence lifetimes for halide sensitive probes are relatively short, as compared to those employed in oxygen sensors, then time-resolved instrumentation costs are typically greater (because of the need for a faster detection system), which is probably one of the main reasons why more attention has been paid to sensing oxygen than halide, given that both are equally as important analytes. However, over the past five years we have seen the welcomed arrival of low cost picosecond diode lasers and nanosecond pulsed light emitting diodes, now covering the visible range, which has helped to reduce instrumentation costs as well as providing us with a greater potential choice of dyes for halide sensing and, coupled with the fact that quenching kinetics of immobilized dye oxygen sensors are fairly well understood, we may soon see similar kinetic interpretations applied to halide sensors and consequently a further expansion of this important field. It is therefore likely that future halide concentrations may be determined with lifetime based, *multiple dye* halide sensors (fibre-optic or implant), where sensors may be constructed with dyes immobilized on the surface of an inert support or fibre, for greater halide sensitivity.

Acknowledgments

The author would like to thank members of the Photophysics Group, Department of Physics and Applied Physics, The University of Strathclyde, Dr Jan Karolin and Professor David J S Birch for informative discussions. The help and guidance of Dr Peter Douglas, Department of Chemistry, University of Wales Swansea, is most gratefully acknowledged.

Glossary of mathematical terms

A	Absorption or acceptor
D	Sum of the diffusion coefficients of quencher and fluorophore, dielectric constant or donor

ϵ_0	Elementary charge
$\epsilon_A(\lambda)$	Extinction coefficient of acceptor at λ
f_a	Fraction of initial fluorescence accessible to quencher
$F_D(\lambda)$	Corrected donor emission spectrum
γ	Quenching efficiency
I_0	Fluorescence intensity in the absence of quencher
I	Fluorescence intensity in the presence of quencher
k	Diffusion limited bimolecular rate constant for collision, $k_q = \gamma k$
K_{APP}	Apparent quenching constant
k_b	Boltzmann's constant
K_{SV}	Stern–Volmer constant for dynamic quenching (K_{SV} is sometimes also referred to as K_D in the research literature, with units of M^{-1} or $mol^{-1} dm^3$).
K_S	Stern–Volmer constant for static quenching
$^O K_{SV}$	Stern–Volmer constant for oxygen
$^H K_{SV}$	Stern–Volmer constant for halothane
k_q	Bimolecular quenching rate constant
k_q^*	Apparent quenching rate constant when considering charge effects on quenching
k_T	Transfer rate in energy transfer
k_{nr}	Non-radiative decay rate
κ^2	Orientation factor in fluorescence resonance energy transfer
λ	Wavelength
$\lambda_{abs} \max$	Absorption wavelength maximum (nm)
$\lambda_{em} \max$	Emission wavelength maximum (nm)
Γ	Radiative decay rate
N^{1000}	Avogadro's number divided by 1000
N	Avogadro's number
n	Refractive index
η	Viscosity
Q	Quencher
Q_D	Donor quantum yield
r	Donor to acceptor distance
R	Radius of quencher or fluorophore
R_0	Förster distance
R_0^a	Sum of molecular radii of quencher and fluorophore
R_0^*	Distance of closest approach of quencher and fluorophore
T	Absolute temperature
τ_0	Fluorescence lifetime in absence of a quencher
τ	Fluorescence lifetime in presence of a quencher
τ_D	Decay time of donor
μ	Ionic strength
V	Quenching sphere volume
Z_0	Charge on quencher near fluorophore
Z_m	Charge on macromolecule near fluorophore

Glossary of acronyms

A^0	Acceptor molecule ground electronic state
A^1	Acceptor molecule first excited singlet state
BTB	Bromothymol blue

CCD	Charge coupled device
F	Fluorophore
FRET	Fluorescence resonance energy transfer (FRET is sometimes also referred to as RET (resonance energy transfer) in the research literature (Lakowicz 1999)).
GFP	Green fluorescent protein
H ₂ DIDS	Dihydro-4,4'-diisothiocyanostilbene-2,2'-disulphonic acid
Harmane	1-Methyl-9H-pyrido[3,4-b]indole (Harmane is sometimes also referred to as Harman or Aribine).
Hb	Haemoglobin
Lucigenin	N,N'-dimethyl-9,9'-bisacridinium nitrate
LZQ	7-(beta-D-ribofuranosylamino)-pyrido [2,1-h]-pteridin-11-ium-5-olate
6MQ	6-methoxy quinoline
6MeQ	6-methyl quinoline
MACA	N-methylacridinium-9-carboxamides
MAMC	N-methylacridinium-9-methylcarboxylate
PTFE	Polytetrafluoroethylene
PVC	Poly(vinyl chloride)
R6G	Rhodamine 6G
RhB	Rhodamine B
S ₀	Fluorophore ground electronic state
S ₁	Fluorophore first excited singlet state
SPA	N-(sulphopropyl) acridinium
SPI	1-methyl-2-(sulphonatopropyl)-9H-pyrido[3,4-b] indolium
SPQ	6-methoxy-N-(3-sulphopropyl) quinolinium
T ₁	Fluorophore first excited triplet state
TPP	Tetraphenylporphyrin
YFP	Yellow fluorescent protein

References

- Aabech H S and Steinnes E 1980 Determination of plasma inorganic iodide by neutron activation analysis after ultrafiltration *Scand. J. Clin. Lab. Invest.* **40** 551–4
- Abramovic B, Horvath K and Gaal F 1993 Automatic titrimetric determination of iodide in some pharmaceutical contrasting preparations *J. Pharmaceut. Biomed. Anal.* **11** 447–50
- Ando T and Asai H 1980 Charge effects on the dynamic quenching of fluorescence of 1,N⁶-ethenoadenosine oligophosphates by iodide, thallium (I) and acrylamide *J. Biochem. (Tokyo)* **88** 255–64
- Andrews-Wilberforce D and Patonay G 1989 Fluorescence quenching studies of near-infrared fluorophores *Appl. Spectr.* **43** 1450–5
- Arai K, Kusu F, Noguchi N, Takamura K and Osawa H 1996 Selective determination of chloride and bromide ions in serum by cyclic voltammetry *Anal. Biochem.* **240** 109–13
- Bacon J R and Demas J N 1987 Determination of oxygen concentrations by luminescence quenching of a polymer immobilized transition metal complex *Anal. Chem.* **59** 2780–5
- Barbour H M 1991 Development and evaluation of the simultaneous determination of sweat sodium and chloride by ion-selective electrodes *Ann. Clin. Biochem.* **28** 150–4
- Barkley R A and Thompson T G 1960 Determination of chemically combined iodine in sea water by amperometric and catalytic methods *Anal. Chem.* **32** 154–8
- Behera P K and Mishra A K 1993 Static and dynamic model for 1-naphthol fluorescence quenching by carbon tetrachloride in dioxane-acetonitrile mixtures *J. Photochem. Photobiol. A* **71** 115–18
- Behera P K, Mukherjee T and Mishra A K 1995a Simultaneous presence of static and dynamic component in the fluorescence quenching of substituted naphthalene–CCl₄ system *J. Lumin.* **65** 131–6
- 1995b Quenching of substituted naphthalenes fluorescence by chloromethanes *J. Lumin.* **65** 137–42
- Berke N S and Hicks M C 1993 Predicting chloride profiles in concrete *Corrosion* 93 paper no 341 (Cambridge, MA: Grace)
- Berry M N, Mazzachi R D and Peake M J 1992 Enzymatic spectrophotometric determination of sodium, potassium and chloride ions in serum or urine *Wiener Klin. Wochenschr.* **104** (S192) 3
- Birch D J S and Imhof R E 1991 Time-domain fluorescence spectroscopy using time-correlated single-photon counting *Topics in Fluorescence Spectroscopy (Vol 1, Techniques)* ed J R Lakowicz (New York: Plenum) pp 1–95
- Birks J B (ed) 1975 *Organic Molecular Photophysics* (New York: Wiley) pp 409–613
- Biwersi J, Tulk B and Verkman A S 1994 Long-wavelength chloride-sensitive fluorescent indicators *Anal. Biochem.* **219** 139–43
- Blick K E and Commens M J 1982 A modified mercury thiocyanate method for the measurement of chloride levels in sweat *Clin. Chem.* **28** 1553
- Boaz H and Rollefson G K 1950 The quenching of fluorescence. Deviations from the Stern–Volmer law *J. Am. Chem. Soc.* **72** 3425–43
- Borissevitch I E 1999 More about the inner filter effect: corrections of Stern–Volmer fluorescence quenching constants are necessary at very low optical absorption of the quencher *J. Lumin.* **81** 219–24
- Bryant C W, Amy G L, Alleman B C and Barkley W A 1990 Measurement of molecular weight distributions of organic halide in kraft mill waste streams, waste solids and pulp *Environ. Technol.* **11** 249–62
- Buchberger W and Huebauer U 1989 Selective determination of bromide and iodide in serum and urine by gas chromatography *Mikrochim. Acta* **3** 137–42
- Buchberger W and Winsauer K 1985 Determination of traces of iodide in serum and urine by ion chromatography *Mikrochim. Acta* **3** 347–52
- Burguera J L, Brunetto M R, Contreras Y, Burguera M, Galignani M and Carrero P 1996 Head-space flow injection for the on-line determination of iodide in urine samples with chemiluminescence detection *Talanta* **43** 839–50
- Butler E C V 1996 The analytical chemist at sea: measurements of iodine and arsenic in marine waters *Trends Anal. Chem.* **15** 45–52
- Carraway E R, Demas J N and DeGraff B A 1991a Luminescence quenching mechanism for microheterogeneous systems *Anal. Chem.* **63** 332–6
- Carraway E R, Demas J N, DeGraff B A and Bacon J R 1991b Photophysics and photochemistry of oxygen sensors based on luminescent transition-metal complexes *Anal. Chem.* **63** 337–42
- Carrigan S, Doucette S, Jones C, Marzocco C J and Halpern A M 1996 The fluorescence quenching of 5,6-benzoquinoline and its conjugate acid by Cl⁻, Br⁻, SCN⁻ and I⁻ ions *J. Photochem. Photobiol. A* **99** 29–35
- Caruana D J 1998 Measurement of the anesthetic agent halothane using an electrochemical-based sensor *Polym. Sensors* **690** 188–208
- Castano F, Lazaro A, Lombrana S and Martinez E 1983 On the fluorescence quenching of pyrene by iodine *Spectrochim. Acta A* **39** 33–5
- Chalfie M, Tu Y, Euskirchen G, Ward W and Prasher D 1994 Green fluorescent protein as a marker for gene expression *Science* **263** 802–5
- Chandramouleeswaran S, Vijayalakshmi B, Kartihkeyan S, Rao T P and Iyer C S P 1998 Ion-chromatographic determination of iodide in sea water with UV detection *Mikrochim. Acta* **128** 75–7

- Charlesworth J M 1994 Optical sensing of oxygen using phosphorescence quenching *Sensors Actuators B* **22** 1–5
- Chen J, Li W, Yan C, Yuan L, Guo J and Zhou X 1997 Characterisation and application of PBA fibre-optic chemical sensor based on fluorescence multiple quenching *Sci. China C* **40** 414–21
- Cheung H C 1991 Resonance energy transfer *Topics in Fluorescence Spectroscopy Vol 2, Principles* ed J R Lakowicz (New York: Plenum) pp 127–76
- Clegg R M 1996 Fluorescence resonance energy transfer *Fluorescence Imaging Spectroscopy and Microscopy* ed X F Wang and B Herman (New York: Wiley) pp 179–252
- Cooper G J S and Croxon M S 1983 Chloride interference with use of an iodide selective electrode for urinary I^- *Clin. Chem.* **29** 1320
- Cosentino P, Grossman C, Shieh C, Doi S, Xi H and Erbland P 1995 Fibre optic chloride sensor development *J. Geotech. Eng.* **121** 610–17
- Cowan D O and Drisko R L E 1970 The photodimerization of acenaphthylene. Heavy atom solvent effects *J. Am. Chem. Soc.* **92** 6281–5
- Cox M E and Dunn B 1985 Detection of oxygen by fluorescence quenching *Appl. Opt.* **24** 2114–20
- Culik B 1986 Microdiffusion and spectrophotometric determination of fluoride in biological samples *Anal. Chim. Acta* **189** 329–37
- Davis G A 1973 Quenching of aromatic hydrocarbons by alkylpyridinium halides *J. Chem. Soc. Chem. Commun.* **1973** 728–9
- Demas J N and DeGraff B A 1994 Design and applications of highly luminescent transition metal complexes *Topics in Fluorescence Spectroscopy, Vol. 4, Probe Design and Chemical Sensing* ed J R Lakowicz (New York: Plenum) pp 71–107
- Deumie M, Baraka M EI and Quinones E 1995 Fluorescence quenching of pyrene derivatives by iodide compounds in erythrocyte membranes: an approach to the probe location *J. Photochem. Photobiol. A* **87** 105–13
- Diprose K V, Epstein H G and Redman L R 1980 An improved ultra-violet halothane meter *Br. J. Anaesth.* **52** 1155–60
- Dueck R, Rathbun N and Wagner P D 1978 Chromatographic analysis of multiple tracer inert gases in the presence of anesthetic gases *Anesthesiology* **49** 31–6
- Dwyer T M and Farley R M 1991 Intracellular chloride in submucosal gland-cells *Life Sci.* **48** 2119–27
- Eder J M 1945 *History of Photography* (New York: Columbia University Press)
- Eftink M R 1991 Fluorescence quenching: theory and applications *Topics in Fluorescence Spectroscopy Vol. 2, Principles* ed J R Lakowicz (New York: Plenum) pp 53–126
- Eftink M R and Ghiron C A 1981 Fluorescence quenching studies with proteins *Anal. Biochem.* **114** 199–227
- Elslinger M A, Wachter R M, Hanson G T, Kallio K and Remington S J 1999 Structural and spectral response of green fluorescent protein variants to changes in pH *Biochemistry* **38** 5296–301
- Fabbrizzi L, Licchelli M, Pallavicini P, Sacchi D and Taglietti A 1996 Sensing of transition metals through fluorescence quenching or enhancement—a review *Analyst* **121** 1763–8
- Förster Th 1948 Intermolecular energy migration and fluorescence *Ann. Phys., Lpz.* **2** 55–75
- Gale P A, Twyman L J, Handlin C I and Sessler J L 1999 A colorimetric calyx[4]pyrrole-4-nitrophenolate based anion sensor *Chem. Commun.* **18** 1851–2
- Garcia C, Lapa R A S, Lima J L F C and Perez-Olmos R 1992 Determination of fluoride in Spanish vinegars *J. Food Chem.* **45** 365–7
- Garcia N H, Plato C F and Garvin J L 1999 Fluorescent determination of chloride in nanoliter samples *Kidney Int.* **55** 321–5
- Geddes C D 2000a Optical thin film polymeric sensors for the determination of aqueous chloride, bromide and iodide ions at high pH, based on the quenching of fluorescence of two acridinium dyes *Dyes Pigments* **45** 243–51
- 2000b A halide sensor based on the quenching of fluorescence of an immobilized indolium salt *Photochem. Photobiol. A* **137** 145–53
- 2001 Halide sensing using the SPQ molecule *Sensors Actuators B* **72** 188–95
- Geddes C D, Apperson K, Karolin J and Birch D J S 2001a Chloride sensitive probes for biological applications *Dyes Pigments* **48** 227–31
- 2001b Chloride sensitive fluorescent indicators *Anal. Biochem.* **293** 60–6
- Geddes C D and Douglas P 2000 Fluorescent dyes bound to hydrophilic copolymers—applications for aqueous halide sensing *Appl. Polym. Sci.* **76** 603–15
- Geddes C D, Douglas P, Moore C P, Wear T J and Egerton P L 1999a New indolium and quinolinium dyes sensitive to aqueous halide ions at physiological concentrations *J. Heterocycl. Chem.* **36** 949–51
- 1999b Optical thin film sensors for the determination of aqueous halide ions *J. Fluoresc.* **9** 163–71
- 1999c A compact optical flow cell for use in aqueous halide determination *Meas. Sci. Technol.* **10** N34–7
- Ghimicescu C, Stan M and Dragomir B 1973 Nouvelle micromethode colorimetrique de dosage de l'ion I^- dans les eaux et les substances organiques *Talanta* **20** 246–7 (in French)
- Gibson L E and Cooke R E 1959 A test for concentration of electrolytes in sweat in cystic fibrosis of the patients utilizing pilocarpine by iontophoresis *Pediatrics* **23** 545–9
- Globel B 1977 Determination of iodine in plasma and biological fluids in the range 2 nmol/L with the aid of an autoanalyser *J. Clin. Chem. Clin. Biochem.* **15** 499–501
- Goewie C E and Hogendoorn E A 1985 Liquid chromatographic determination of bromide in human milk and plasma *J. Chromatogr.* **344** 157–65
- Gonzalez M A, Aller A J, Pardo R, Barrado E and Deban L 1991 Fluoride and chloride determination in cheese with ion-selective electrodes *Electroanalysis* **3** 439–42
- Greco F A and Solomon A K 1997 Kinetics of chloride–bicarbonate exchange across the human red blood cell membrane *J. Membrane Biol.* **159** 197–208
- Hall E A H, Conhill E J and Hahn C E W 1988 Halothane interference at an amperometric oxygen-electrode—the development of an oxygen halothane sensor *J. Biomed. Eng.* **10** 319–25
- Hattab F N 1987 Direct determination of fluoride in selected dental materials *Dent. Mater.* **3** 67–70
- 1989 Analytical methods for the determination of various forms of fluoride in toothpastes *J. Dent.* **17** 77–83
- Heim R and Tsien R Y 1996 Engineering green fluorescent protein for improved brightness, longer wavelengths and fluorescence resonance energy transfer *Curr. Biol.* **6** 178–82.
- Howie J A B and Hawkins P 1993 Fast-responding, fibre-optic based sensing system for the volatile anaesthetic halothane, using an ultraviolet absorption technique and a fluorescent film *Analyst* **118** 35–40
- Huber C, Werner T, Krause C, Klimant I and Wolfbeis O S 1998 Energy transfer-based lifetime sensing of chloride using a luminescent transition metal complex *Anal. Chim. Acta* **364** 143–51
- Ikenishi R and Kitagawa T 1988 Gas chromatographic method for the determination of fluoride ion in biological samples II. Stability of fluoride-containing drugs and compounds in human plasma *Chem. Pharm. Bull.* **36** 810–14
- Illsley N P and Verkman A S 1987 Membrane chloride transport measured using a chloride-sensitive fluorescent probe *Biochem.* **26** 1215–19
- Jayaraman S, Biwersi J and Verkman A S 1999a Synthesis and characterisation of dual-wavelength Cl^- sensitive fluorescent indicators for ratio imaging *Am. J. Phys. Cell Phys.* **45** C747–57
- Jayaraman S, Haggie P, Wachter R M, Remington S J and Verkman A S 2000 Mechanism and cellular applications of a green fluorescent protein-based halide sensor **275** 6047–50

- Jayaraman S, Teitler L, Skalski B and Verkman A S 1999b Long-wavelength iodide-sensitive fluorescent indicators for measurement of functional CFTR expression in cells *Am. J. Phys. Cell Phys.* **277** C1008–18
- Jayaraman S and Verkman A S 2000 Quenching mechanism of quinolinium type chloride-sensitive fluorescent indicators *Biophys. Chem.* **85** 49–57
- Jiwan H J-L and Soumillion J-Ph 1997 A halogen anion sensor based on the hydrophilic entrapment of a fluorescent probe in silica sol-gel thin films *J. Non-Cryst. Solids* **220** 316–22
- Jones S D, Spencer C P and Truesdale V W 1982 Determination of total iodine and iodate-iodine in natural freshwater *Analyst* **107** 1417–24
- Kaplan N M, Simons M and McPhee C 1982 Two techniques to improve adherence to dietary sodium restriction in the treatment of hypertension *Arch. Intern. Med.* **142** 1638–41
- Kautsky H 1939 Quenching of luminescence by oxygen *Trans. Faraday Soc.* **35** 216–19
- Keizer J 1983 Non-linear fluorescence quenching and the origin of positive curvature in Stern–Volmer plots *J. Am. Chem. Soc.* **105** 1494–8
- Kerem B, Rommens J A, Buchanan J A, Markiewicz D, Cox T K, Chakravarti A, Buckwald M and Tsui L C 1989 Identification of the cystic fibrosis gene: genetic analysis *Science* **245** 1073–80
- Kissa E 1987 Determination of inorganic fluoride in blood with a fluoride ion-selective electrode *Clin. Chem.* **33** 253–5
- Kisters K, Tepel M, Hahne G, Wibbeke C, Spieker C and Zider W 1997 Chloride concentrations in plasma, erythrocytes and lymphocytes indicating different chloride fluxes: measurements using SPQ and colorimetric titration *Trace Elements Electrolytes* **14** 55–7
- Koch S M and Taylor R W 1992 Chloride ion in intensive care medicine *Crit. Care Med.* **20** 227–40
- Komaromy-Hiller G, Swallow K L and Moulton L 1998 Inadequate measurement of urinary chloride *Ann. Clin. Lab.* **28** 347–53
- Krapf R, Illsley N P, Tseng H C and Verkman A S 1988 Structure–activity relationships of chloride-sensitive fluorescent indicators for biological application *Anal. Biochem.* **169** 142–50
- Kreingol'd S U 1983 *Catalymetry in Analysis of Reagents and Especially Pure Substances* (Moscow: Khimiya) p 136
- Labiana D A, Taylor G N and Hammond G S 1972 Structure reactivity factors in the quenching of fluorescence from naphthalenes by conjugated dienes *J. Am. Chem. Soc.* **94** 3679–83
- Lakowicz J R (ed) 1995 *Proc. SPIE* **2388**
- (ed) 1997 *Topics in Fluorescence Spectroscopy, Non-Linear and Two Photon Induced Fluorescence* vol 5 (New York: Plenum)
- 1999 *Principles of Fluorescence Spectroscopy* 2nd edn (New York: Kluwer–Plenum)
- Lakowicz J R and Gryczynski I 1991 Frequency-domain fluorescence spectroscopy *Topics in Fluorescence Spectroscopy, Vol. 1, Techniques* ed J R Lakowicz (New York: Plenum) pp 293–335
- Lakowicz J R and Weber G 1973 Quenching of fluorescence by oxygen. A probe for structural fluctuations in macromolecules *Biochemistry* **12** 4161–70
- Lamb M D 1978 *Luminescence Spectroscopy* (New York: Academic) pp 93–148
- Lawrence J F, Chadha R K and Conacher H B S 1983 The use of ion-exchange filters for the determination of iodide in milk by x-ray fluorescence spectrometry *Int. J. Environ. Anal. Chem.* **15** 303–8
- Laws W R and Contino P B 1992 Fluorescence quenching studies: analysis of non-linear Stern–Volmer data *Methods Enzymol.* **220** 448–63
- Leaback D H 1997 Sir George Stokes, Cambridge and the nature of fluorescence processes *J. Fluoresc.* **7** 3S–5S (supplement)
- Leeuwen van F X R and Sangster B 1987 The toxicology of the bromide ion *CRC Crit. Rev. Toxicol.* **18** 189–213
- Lehrer S S 1971 Solute perturbation of protein fluorescence. The quenching of the tryptophan fluorescence of model compounds and of lysozyme by iodide ion *Biochemistry* **10** 3254–63
- (ed) 1976 *Biochemical Fluorescence Concepts* vol 2 (New York: Dekker) p 515
- Lippitsch M E, Draxler S and Kieslinger D 1997 Luminescence lifetime-based sensing: new materials, new devices *Sensors Actuators B* **38/39** 96–102
- Luft F C, Fineberg N S and Sloan R S 1982 Overnight urine collections to estimate sodium intake *Hypertension* **4** 494–8
- Mac M, Wach A and Najbar J 1991 Solvent effects on the fluorescence quenching of anthracene by iodide ions *Chem. Phys. Lett.* **176** 167–72
- Makowetz E, Muller K and Spitzzy H 1966 Separation and determination of thyroid hormones in the nanogram range based on the sorption of properties of Sephadex *J. Microchem.* **10** 194–201
- Mark H and Rechnitz G 1968 *Kinetics in Analytical Chemistry* (New York: Wiley)
- Martin A and Narayanaswamy R 1997 Studies on quenching of fluorescence of reagents in aqueous solution leading to an optical chloride-ion sensor *Sensors Actuators B* **38/39** 330–3
- Mayrhofer R C and Betts T A 1998 Fluorescence quenching of quinine with halide ions *Abstr. Papers Am. Chem. Soc.* **216** 125-ched
- Melhem M F, Seltman H and Sanghvi A 1985 Measurement of urinary chloride with the Kodak Ektachem 400 *Clin. Chem.* **31** 599–600
- Mersin S S, Ramelli G P, Laux-End R and Bianchetti M G 1995 Urinary chloride excretion distinguishes between renal and extrarenal metabolic alkalosis *Eur. J. Pediatr.* **154** 979–82
- Michalke B, Schramel P and Hasse S 1996 Determination of free iodide in human serum: separation from other I-species and quantification in serum pools and individual samples *Mikrochim. Acta* **122** 67–76
- Michigami Y, Kuroda Y, Ueda K and Yamamoto Y 1993 Determination of urinary fluoride by ion chromatography *Anal. Chim. Acta* **274** 299–302
- Miller M E and Cappon C J 1984 Anion-exchange chromatographic determination of bromide in serum *Clin. Chem.* **30** 781–3
- Mills A 1998a Controlling the sensitivity of optical oxygen sensors *Sensors Actuators B* **51** 60–8
- 1998b Optical sensors for oxygen: a log-gaussian multisite-quenching model *Sensors Actuators B* **51** 69–76
- 1999a Response characteristics of optical sensors for oxygen: models based on a distribution in tau or kappa *Analyst* **124** 1301–7
- 1999b Response characteristics of optical sensors for oxygen: models based on a distribution in tau or kappa *Analyst* **124** 1309–14
- Mills A and Williams F C 1997 Chemical influences on the luminescence of ruthenium diimine complexes and its response to oxygen *Thin Solid Films* **306** 163–70
- Miyawaki A, Griesbeck O, Heim R and Tsien R Y 1999 Dynamic and quantitative Ca²⁺ measurements using improved cameleons *Proc. Natl Acad. Sci. USA* **96** 2135–40
- Momin S A and Narayanaswamy R 1992 Quenching of fluorescence of polynuclear aromatic hydrocarbons by chlorine *Analyst* **117** 83–5
- Moriya T 1984 Excited-state reactions of coumarins in aqueous solutions II. The fluorescence quenching of 7-ethoxycoumarins by halide ions *Bull. Chem. Soc. Japan* **57** 1723–30
- 1986 Excited-state reactions of coumarins in aqueous solutions III. The fluorescence quenching of 7-ethoxycoumarins by the chloride ion in acidic solutions *Bull. Chem. Soc. Japan* **59** 961–8
- 1988 Excited-state reactions of coumarins in aqueous solutions VI. The fluorescence quenching of 7-hydroxycoumarins by chloride ions in acidic solutions *Bull. Chem. Soc. Japan* **61** 753–9
- Moussa F, Raux-Demay M, Vienberg F, Depasse F, Gharbi R, Hautem J-Y and Aymard P 1995 Determination of iodide in

- serum and urine by ion-pair reversed-phase high-performance liquid chromatography with coulometric detection *J. Chromatogr. B* **667** 69–74
- Muller K 1967 Simple method for the determination of the distribution of ^{131}I in blood serum *Clin. Chim. Acta* **17** 21–9
- Mura P, Papet Y, Sanchez A and Piriou A 1995 Rapid and specific high-performance liquid chromatographic method for the determination of iodide in urine *J. Chromatogr. B* **664** 440–3
- Naim J O, Lanzafame R J, Blackman J R and Hinshaw R J 1986 The *in vitro* quenching effects of iron and iodine on fluorescein fluorescence *J. Surg. Res.* **40** 225–8
- Najbar J and Mac M 1991 Mechanisms of fluorescence quenching of aromatic molecules by potassium iodide and potassium bromide in methanol–ethanol solutions *J. Chem. Soc. Faraday Trans* **87** 1523–9
- Nathanson I, Tucker M and Jones L 1994 Measurement of chloride concentration in microvolume samples of sweat *Pediatr. Pulmonol.* **17** 340–2
- 1995 On the measurement of chloride concentration in microvolume samples of sweat *Pediatr. Pulmonol.* **19** 66–8
- Noyes R M 1961 Effects of diffusion rates on chemical kinetics *Prog. React. Kinet.* **1** 29–60
- Okamoto M 2000 Kinetic study of the external heavy-atom quenching of fluorescence in liquid solution under high pressure *J. Phys. Chem. A* **104** 7518–24
- Okamoto M and Teranishi H 1984 Effect of pressure on the external heavy-atom quenching of pyrene fluorescence in fluid solution *J. Phys. Chem.* **88** 5644–6
- Palm G J and Wlodawer A 1999 Spectral variants of green fluorescent protein *Methods Enzymol.* **302** 378–94
- Peterson J L, Fitzgerald R V and Buckhold D K 1984 Fibre-optic probe for *in vivo* measurement of oxygen partial pressure *Anal. Chem.* **56** 62–7
- Pilas B and Durack G 1997 A flow cytometric method for measurement of intracellular chloride concentration in lymphocytes using the halide specific probe 6-methoxy-N-(3-sulphopropyl) quinolinium (SPQ) *Cytometry* **28** 316–22
- Postmes T J and Coenegracht J M 1972 A chemical determination of plasma inorganic iodide by ultrafiltration *Clin. Chim Acta* **38** 313–19
- Potter J J, Hilliker A E and Breen G J 1986 Determination of fluoride and monofluorophosphate in toothpastes by ion chromatography *J. Chromatogr.* **367** 423–7
- Prasad A S 1978 *Trace Elements and Iron in the Human Metabolism* (New York: Plenum)
- Preuss H G 1993 Fundamentals of clinical acid–base evaluation *Clin. Lab. Med.* **13** 103–16
- Rendl J, Seybold S and Borner W 1994 Urinary iodide determined by paired-ion reversed-phase HPLC with electrochemical detection *Clin. Chem.* **40** 908–13
- Richards-Kortum R and Sevick-Muraca E 1996 Quantitative optical spectroscopy for tissue diagnosis *Annu. Rev. Phys. Chem.* **47** 555–606
- Riggin R M, Lucas S V, Jungclaus G A and Billets S 1984 Measurement of organic halide content of aqueous and solid waste samples *J. Testing Eval.* **12** 91–9
- Risley D S, Peterson J A, Griffiths K L and McCarthy S 1996 An alternative method for the determination of chloride in pharmaceutical drug substances using HPLC and evaporative light scattering *LC GC-Mag. Separation Sci.* **14** 1040–7
- Sandulescu R, Florean E, Roman L, Mirel S, Oprean R and Suciuc P 1996 Spectrophotometric determination of fluoride in dosage forms and dental preparations *J. Pharmaceut. Biomed. Anal.* **14** 951–8
- Sarpal R S and Dogra S K 1994 Fluorescence quenching of a few aromatic-amines by inorganic anions *Indian J. Chem. A* **33** 111–14
- Seifert K, Dominok B and Dominok G W 1986 Improved methods for determination of fluoride in biological materials *Fluoride* **19** 22–5
- Sharma A, Draxler S and Lippitsch M E 1992 Time resolved spectroscopy of the fluorescence quenching of a donor-acceptor pair by halothane *Appl. Phys. B* **54** 309–12
- Sharpe A G 1990 The solvation of halide ions and its chemical significance *J. Chem. Ed.* **67** 309–15
- Sherman R A and Faustino E F 1987 Bedside urinary chloride measurement *Am. J. Emerg. Med.* **5** 52–3
- Sivaraman C P and Rajeswari S 1983 Determination of iodide and iodate in seawater *Indian J. Marine Sci.* **12** 177–80
- Sloan P J M, Beavers G and Baxter F E 1984 The Quantab strip in the measurement of urinary chloride and sodium concentrations *Clin. Chem.* **30** 1705–7
- Srinivas S P, Bonanno J A and Hughes B A 1998 Assessment of swelling-activated Cl^- channels using the halide sensitive fluorescent indicator 6-methoxy-N-(3-sulphopropyl) quinolinium *Biophys. J.* **75** 115–23
- Steinberg I Z 1971 Long-range nonradiative transfer of electronic excitation energy in proteins and polypeptides *Annu. Rev. Biochem.* **40** 83–114
- Stern O and Volmer M 1919 Uber die abklingungszeit der fluoreszenz *Phys. Z.* **20** 183–8 (in German)
- Stokes G G 1869 On a certain reaction of quinine *J. Chem. Soc.* **22** 174–85
- Stryer L 1978 Fluorescence resonance energy transfer as a spectroscopic ruler *Annu. Rev. Biochem.* **47** 819–46
- Sullivan K F and Kay S A E 1999 Green fluorescent proteins *Methods in Cell Biology* vol 58 (San Diego: Academic)
- Sung J, Shin K J and Lee S 1992 Theory of diffusion-influenced fluorescence quenching. Effects of static quenching on the Stern–Volmer curve *Chem. Phys.* **167** 17–36
- 1994 Theory of diffusion-influenced fluorescence quenching—effects of static quenching on the Stern–Volmer curve *Chem. Phys.* **185** 413
- Suptitz P 1996 The impact of solid state physics on silver halide photography—a historical review *J. Inf. Recording* **23** 227–32
- Szmacinski H and Lakowicz J R 1994 Lifetime-based sensing *Topics in Fluorescence Spectroscopy, Vol. 4, Probe Design and Chemical Sensing* ed J R Lakowicz (New York: Plenum) pp 295–334
- Tani T 1995 The present status and future prospects of silver halide photography *J. Imaging Sci. Technol.* **39** 31–40
- 1998 Progress and future prospects of silver halide photography compared with digital imaging *J. Imaging Sci. Technol.* **42** 1–14
- Taylor R P and James T J 1997 Enzymatic measurement of sweat sodium chloride *Ann. Clin. Biochem.* **34** 211
- Thompson R B (ed) 1997 *Proc. SPIE* **2980**
- Tsien R Y 1998 The green fluorescent protein *Annu. Rev. Biochem.* **67** 509–44
- Tsikis D, Fauler J and Frolich J C 1992 Determination of chloride in biological fluids as pentafluorobenzylchloride by reverse phase high performance liquid chromatography and UV detection *Chromatographia* **33** 317–20
- Tucker S A and Acree W E 1995 Analytical method for the simultaneous determination of chloride and bromide ions, based upon fluorescence quenching methods *J. Chem. Ed.* **72** A31–3
- Turro N J 1991 *Modern Molecular Photochemistry* (Sausalito, CA: University Science Books)
- Turzo A, Legendre J M, Quiniou R and Morin P P 1990 Iodide urinary measurement by x-ray fluorescence *Ann. Biol. Clin.* **48** 627–30
- Tyler J E and Poole D F G 1989 The rapid measurement of fluoride concentrations in stored human saliva by means of a differential electrode cell *Arch. Oral Biol.* **34** 995–8
- Tyler J E, Poole D F G and Kong K L 1988 Determination of fluoride in blood plasma *J. Dent. Res.* **67** 677
- Urbano E, Offenbacher H and Wolfbeis O S 1984 Optical sensor for continuous determination of halides *Anal. Chem.* **56** 427–9
- Verity B and Bigger S W 1996 The dependence of quinine fluorescence quenching on ionic strength *Int. J. Chem. Kinet.* **28** 919–23

- Versieck J and Cornelis R 1980 Normal levels of trace elements in human blood plasma *Anal. Chim. Acta* **116** 217–54
- Vijan P N and Alder B 1984 Determination of fluoride in vegetation by ion-selective electrode *Am. Lab.* **16** 16–24
- Volkmer A, Hatrick D A and Birch D J S 1997 Time-resolved nonlinear fluorescence spectroscopy using femtosecond multiphoton excitation and single-photon timing detection *Meas. Sci. Technol.* **8** 1339–47
- Wachter R M and Remington S J 1999 Sensitivity of the yellow variant of green fluorescent protein to halides and nitrate *Curr. Biol.* **9** R628–9
- Wachter R M, Yarbrough D, Kallio K and Remington S J 2000 Crystallographic and energetic analysis of binding of selected anions to the yellow variants of green fluorescent protein *J. Mol. Biol.* **301** 157–71
- Ware W R 1962 Oxygen quenching of fluorescence in solution: an experimental study of the diffusion process *J. Phys. Chem.* **66** 455–8
- Warwick J W, Huang N N, Waring W W, Cherian A G, Brown I, Stejskal-Lorenz E, Yeung W H, Duhon G, Hill J G and Strominger D 1986 Evaluation of a cystic fibrosis screening system incorporating a miniature sweat stimulator and disposable chloride sensor *Clin. Chem.* **32** 850–3
- Washington K, Sarasua M M, Koehler L S, Koehler K A, Schultz J A, Pedersen L G and Hiskey R G 1984 Utilization of heavy-atom effect quenching of pyrene fluorescence to determine the intramembrane distribution of halothane *Photochem. Photobiol.* **40** 693–701
- Watkins A R 1974 Kinetics of fluorescence quenching by inorganic anions *J. Phys. Chem.* **78** 2555–8
- Wegman D, Weiss H, Ammann D, Morf W E, Pretsch E, Sugahara K and Simon W 1984 Anion-selective electrodes based on lipophilic quaternary ammonium compounds *Microchim. Acta* **3** 1–16
- Weller A 1961 Fast reactions of excited molecules *Prog. React. Kinet.* **1** 187–214
- White R A, Kutz K J and Wampler J E 1991 Fundamentals of fluorescence microscopy *Topics in Fluorescence Spectroscopy, Vol. 1, Techniques* ed J R Lakowicz (New York: Plenum) pp 379–410
- Winter S D 1981 Measurement of urinary electrolytes: clinical significance and methods *Crit. Rev. Clin. Lab. Sci.* **14** 163–87
- Wolfbeis O S (ed) 1991 *Fibre Optic Chemical Sensors and Biosensors* vols 1 and 2 (Boca Raton, FL: Chemical Rubber Company)
- Wolfbeis O S and Hochmuth P 1984 A new method for the endpoint determination in argentometry using halide sensitive fluorescent indicators and fibre optic light guides *Mikrochim. Acta* **3** 129–48
- Wolfbeis O S, Posch H E and Kroneis H W 1985 Fiber optical fluorosensor for determination of halothane and/or oxygen *Anal. Chem.* **57** 2556–61
- Wolfbeis O S and Urbano E 1982 Standards for fluorescence measurements in the near neutral pH range *J. Heterocycl. Chem.* **19** 841–3
- 1983 Fluorescence quenching method for determination of two or three components in solution *Anal. Chem.* **55** 1904–6
- Wong G T F 1991 The marine geochemistry of iodine *Rev. Aquat. Sci.* **4** 45–73
- Wood R E, Boat T F and Doershuk C F 1976 Cystic fibrosis *Am. Rev. Respir. Dis.* **113** 833–78
- Wyatt W A, Bright F V and Hieftje G M 1987 Characterisation and comparison of 3 fibre optic sensors for iodide determination based on dynamic fluorescence quenching of rhodamine 6G *Anal. Chem.* **59** 2272–6
- Xu W, Kneas K A, Demas J N and DeGraff B A 1996 Oxygen sensors based on luminescence quenching of metal complexes: Osmium complexes suitable for laser diode excitation *Anal. Chem.* **66** 4133–41
- Yang R-H, Wang K-M, Xiao D and Yang X-H 2000 Development of an iodine sensor based on fluorescence energy transfer *Analyst* **125** 1441–5
- Yasinskene E I and Umbrazhyunaite O P 1973 Application of dyes for the kinetic determination of ions *Zh. Anal. Khim.* **28** 2025–8 (in Russian)
- Yu B S, Po C, Nie L H and Yao S Z 1996 Determination of chloride in human body fluids by ion chromatography with piezoelectric sensor as detector *Anal. Lett.* **29** 43–57
- Zhang J, Rock D P, Chateaufneuf J E and Brennecke J F 1997 A steady-state and time-resolved study of quenching reactions of anthracene and 1,2 benzanthracene by carbon tetrabromide and bromoethane in supercritical carbon dioxide *J. Am. Chem. Soc.* **119** 9980–91
- Zhu C, Bright F V and Hieftje G M 1990 Simultaneous determination of Br⁻ and I⁻ with a multiple fibre-optic fluorescence sensor *Appl. Spectrosc.* **44** 59–63